2-1-2018

Unequal error protection for power line communications over impulsive noise channels

Osama Senam Mostafa Ali

Follow this and additional works at: https://fount.aucegypt.edu/etds

Recommended Citation

APA Citation
Ali, O. (2018).*Unequal error protection for power line communications over impulsive noise channels* [Master's Thesis, the American University in Cairo]. AUC Knowledge Fountain.
https://fount.aucegypt.edu/etds/636

MLA Citation
Ali, Osama Senam Mostafa. *Unequal error protection for power line communications over impulsive noise channels*. 2018. American University in Cairo, Master's Thesis. *AUC Knowledge Fountain*.
https://fount.aucegypt.edu/etds/636

THE AMERICAN UNIVERSITY IN CAIRO

SCHOOL OF SCIENCES AND ENGINEERING

MASTERS THESIS

Unequal Error Protection for Power Line Communications over Impulsive Noise Channels

Author:
Osama Senam Mostafa Ali

Supervisor:
Dr.Karim Seddik, Dr.Ayman Elezabi

A thesis submitted in fulfillment of the requirements

for the degree of Master of Science

in the department of

Electronics and Communication Engineering

January 2018

THESIS PROPOSAL APPROVAL

Student Full Name: _____

Student ID: _____

Thesis Title: _____

Please attach the thesis proposal to this form.

Proposed Graduation Date: _____

Thesis title and proposal have been approved:

<u>Thesis Supervisor</u>:
Name: _____
Title: _____
Department: _____
Institution: _____
Signature: _____Date: _____

<u>First reader</u>:
Name: _____
Title: _____
Department: _____
Institution: _____
Signature: _____Date: _____

<u>Second reader</u>:
Name: _____
Title: _____
Department: _____
Institution: _____
Signature: _____Date: _____

<u>Department Chair</u>:
Name: _____
Title: _____
Signature: _____Date: _____

<u>Student</u>:
I, (Student Name) _____
have read and understood the thesis guidelines.
Signature: _____Date: _____

Acknowledgements

Abstract

Master of Science

Unequal Error Protection for Power Line Communications over Impulsive Noise Channels

by Osama Senam Mostafa Ali

Power line communication (PLC) has recently attracted a lot of interest with many application areas including smart grids' data communication, where data (from sensors or other measurement units) with different QoS may be transmitted. Power line communications suffer from the excessive power lines' impulsive noise (which can be caused by shedding loads on and off). In this thesis, we present a study of power line communications with unequal error protection for two and four data priority levels hierarchical QAM modulation and space-time block coding. We consider the two commonly used power lines' impulsive noise models with Bernoulli and Poisson arrivals. In our proposed approaches, we achieve UEP on both of bit and symbol levels. Approximate closed-form expressions for the error rates are derived for each priority level for both single carrier and OFDM in SISO and MIMO systems. In addition, these simplified expressions are used to implement a bit loading algorithm to provide UEP for frequency-selective PLC channels.

For the case of MIMO PLC channels, we describe three different MIMO schemes to allow more control over the UEP levels. The three schemes are namely: maximum ratio combiner (MRC) receive diversity, Alamouti space-time block code, and a new structure for a space-time code that allows for unequal error protection at the symbol level. Finally, we apply an Eigen beamforming technique, assuming channel knowledge at transmitter, which improves the BER as compared to the other MIMO PLC schemes.

Contents

List of Figures

List of Tables

Abbreviations

NIST	National Institute of Standards and Technology
EV	Electric Vehicles
SG	Smart Grid
ESI	Energy Services Interface
PLC	Power Line Communication
DLC	Direct Load Control
PMU	Phasor Measurement Units
SCADA	Supervisory Control and Data Acquisition
DER	Distributed Energy Resources
ES	Electricity Supplier
SM	Smart Meter
QoS	Quality of Service
PSD	Power Spectral Density
LTI	Linear Time Invariant
LPTV	Linear Periodically Time-Varying
QAM	Quadrature Amplitude Modulation
UEP	Unequal Error Protection
OFDM	Orthogonal Ffrequency-Division Multiplexing
AWGN	Additive White Gaussian Noise
pdf	probability density function
BER	Bit Error Rate
DFT	Discrete Fourier Transform
erfc	error function complementary
P	phase
N	Neutral

PE	**P**rotective **E**arth
MIMO	**M**ultiple-**I**nput **M**ultiple-**O**utput
SISO	**S**ingle-**I**nput **S**ingle-**O**utput
MRC	**M**aximal **R**atio **C**ombining
HV	**H**igh **V**oltage
MV	**M**edium **V**oltage

Chapter 1

Introduction

1.1 Smart Grid

The current electric power grid depends on different energy sources and the use of renewable energy sources is increasing to reduce the dependence on fossil fuels which pollute the environment heavily and are being consumed rapidly. There is a critical need for intelligent management between different elements in the smart grid as it allows two-way communication between the electric utility and customers to manage the electricity consumption especially at peak hours, so blackouts can be avoided [1]. The National Institute of Standards and Technology (NIST) [2] defined the smart grid as " a planned grid that uses digital computing and communication technologies with the power-delivery infrastructure enabling bidirectional flows of energy and two-way communication and control capabilities will lead to an array of new functionalities and applications ". Electric transportation is an example of these new applications in which electric vehicles (EV) offer the potential to function as energy storage devices, thus playing a unique role in balancing demands on the Smart Grid. NIST constructed a model for a smart grid (SG) in which the grid is divided into seven domains; each domain includes SG actors and applications as illustrated in Table 1.1.

The interaction between actors in different domains is done through secure communication as shown in Fig. 1.1.

TABLE 1.1: Domains and Actors in the Smart Grid Conceptual Model [2]

•	Domain	Description
1	Customer	The end users of electricity. May also generate, store, and manage the use of energy. Traditionally, three customer types are discussed, each with its own sub -domain: home, commercial/building, and industrial.
2	Markets	The operators and participants in electricity markets.
3	Service Provider	The organizations providing services to electrical customers and to utilities.
4	Operations	The managers of the movement of electricity.
5	Bulk Generation	The generators of electricity in bulk quantities. May also store energy for later distribution.
6	Transmission	The carriers of bulk electricity over long distances. May also store and generate electricity.
7	Distribution	The distributors of electricity to and from customers. May also store and generate electricity.
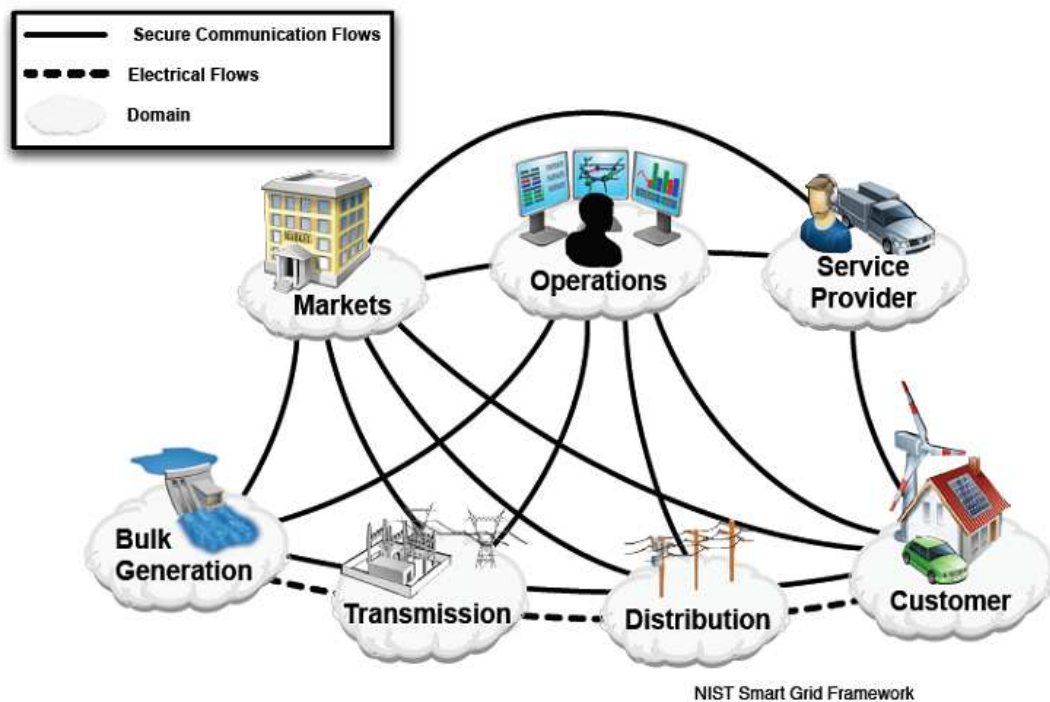
FIGURE 1.1: Interaction of Actors in Different Smart Grid Domains through Secure Communication [2].

1.1.1   Smart Grid Domains

NIST divided the smart grid conceptual model into seven main domains where each domain includes many different applications and actors involved.

1.1.1.1   Customer domain

It includes home,building and industrial subdomains. Actors in this domain enable customers to manage their energy usage and generation because customers will be enabled to provide the grid with electricity as well. Also,control and information flow is enabled between the customer and other domains. The boundaries of this domain are the utility meter and the energy services interface (ESI) which is used for interactions between utility and the customer. Many applications are available within this domain such as home automation which controls different functions in a building, besides remote load control and in-home display of customer usage. Also, industrial automation can be applied to control industrial processes and application of Micro-generation is included which allows monitoring and control of distributed generation.

1.1.1.2   Markets domain

It is the domain where the grid assets are bought and sold. It includes many applications such as market management,retailing,trading and the main business of some companies is buying and selling of energy.

1.1.1.3   Service provider domain

Actors in this domain do services to support the business process of the power system starting from producers to distributors until reaching customers. Examples of these services are billing,customer account management,management of energy use and home energy generation. This domain enables the development of a growing market for third parties to provide value-added services to customers. Also, it enables a decrease in power consumption and increase in power generation because customers become involved actively in the power delivery process. This domain include many applications such as customer management, installation, maintenance, billing and emergency services.

1.1.1.4 Operations domain

Actors in this domain are responsible for the smooth operation of the power system through performing operations such as network monitoring, control, analysis and planning of communication networks.

1.1.1.5 Bulk Generation domain

Electricity generation includes different categories, there is variable generation like from wind and non-variable generation like from coal. Also, they can be classified into renewable and non-renewable sources of generation.

1.1.1.6 Transmission domain

The main responsibility of the transmission operator is to maintain stability on the power grid by balancing supply with demand. Monitoring of the transmission network is controlled by SCADA system.

1.1.1.7 Distribution domain

It represents the electrical interconnection between transmission and customer domains. Also, it communicates with the operations domain to manage power flows.

1.1.2 Smart Grid Applications

[3] determined six categories for smart grid applications and suggested their communication requirements as follow.

1.1.2.1 Advanced Metering Infrastructure

It enables consumers to monitor and control their home appliances remotely. Also, consumers can view their energy consumption and real-time electricity pricing to improve energy efficiency. Communication technologies which are recommended for this application are PLC, WIMAX, cellular.

1.1.2.2 Demand Response

The price of electricity is changing according to peak hours and this price is continuously delivered to the consumer who has the option to power down some of the appliances manually or use direct load control (DLC).

1.1.2.3 Wide-Area Situational Awareness

The power system across large areas should be monitored effectively to provide grid operators with a dynamic picture of the grid functionality. Phasor measurement units (PMUs) and SCADA systems are used in this application where fiber optics and broadband over power lines are recommended communication technologies.

1.1.2.4 Distributed Energy Resources and Storage

It enables the integration of Distributed Energy Resources (DER) into the grid where the energy flow will be multi-directional across the utility and consumers. Also, islanding and balancing of DER will be allowed in smart grid where satellite and microwave are from the recommended technologies.

1.1.2.5 Electric Transportation

Charging of electric vehicles (EV) is a very important application that can also be a source for energy storage and coordination within the grid should be done to avoid overloading. The recommended communication technologies are ZigBee, cellular and PLC.

1.1.2.6 Distribution Grid Management

It targets to isolate potential faults, so that they do not affect other parts of the grid where SCADA provides voltage and current measurements at critical nodes. The recommended communication technologies are fiber optics, cellular and satellite.

Communications requirements of Smart Grid applications are summarized in Table 1.2.

Application	Network Requirements				
	Bandwidth	**Latency**	**Reliability**	**Security**	**Backup Power**
AMI	10-100 kbps/node, 500 kbps for backhaul	2-15 sec	99-99.99%	High	Not necessary
Demand Response	14kbps- 100 kbps per node/device	500 ms- several minutes	99-99.99%	High	Not necessary
Wide Area Situational Awareness	600-1500 kbps	20 ms-200 ms	99.999- 99.9999%	High	24 hour supply
Distribution Energy Resources and Storage	9.6-56 kbps	20 ms-15 sec	99-99.99%	High	1 hour
Electric Transportation	9.6-56 kbps, 100 kbps is a good target	2 sec-5 min	99-99.99%	Relatively high	Not necessary
Distribution Grid Management	9.6-100 kbps	100 ms-2 sec	99-99.999%	High	24-72 hours

TABLE 1.2: Communications requirements of Smart Grid applications [3]

It is clear that a fast, reliable and secure communication network must manage this smart power system. This network is required to connect electric devices in different locations and exchange their data; the communication and network infrastructure should be able to meet reliability and security requirements of the smart grid. It is required that an electricity supplier (ES) measure the electric power consumption of all customers within its region to know the current total power load every small time period using a smart meter (SM). This makes the ES able to estimate the electric consumption profile over different time periods and accordingly provide its customers with information about peak hours and time tariff in order to reduce power consumption and minimize blackout probability. Also, an ES needs to know each customer's power consumption over a certain fixed time period for billing purposes. It is needed to keep the customers' detailed consumption data away from the ES to preserve their privacy because much private information can be revealed from the electric consumption profile such as the presence or absence of residents and the kind of electric device in current usage.

The importance of power line communications is increasing nowadays especially after the emergence of smart grid as an upgrade of the traditional electric power grid. The smart grid involves many applications that take advantage of the existing power lines

TABLE 1.3: PLC technologies

	Ultra Narrow Band	Narrow Band	Broad Band
Data rate	100 bps	up to 500 kbps	up to several hundred Mbps
Frequency Band	0.3–3 kHz 30-300 Hz	3–500 kHz	1.8–250 MHz
Standards	TWACS	PRIME G3-PLC ITU-T G.hnem IEEE 1901.2	TIA-1113 IEEE 1901

for communication between different nodes. For example, it allows intelligent management between the electric utility and the customers through two-way communication to manage the electricity consumption especially at peak hours, so blackouts can be avoided [1]. Also, it allows many indoor applications over power lines such as Internet access and home automation. The data transmitted over power lines can have different required quality of service (QoS), and hierarchical modulation may be utilized to give more protection to the highest priority data. For example, the communication between the customer and the utility might have a more stringent QoS requirement as compared to Internet access or some home automation data.

1.2   Power Line Communication

Electric utilities have been using power line communication technology for remote metering and load control; at first single carrier narrow band solutions were used then broadband systems started to appear as technology advanced reaching rates of 200 Mbps [4]. PLC technologies can be classified as shown in Table 1.3.

Today PLC is widely used in smart grid for high voltage, medium voltage and low voltage networks. There are PLC technologies in the 40-500 KHZ band which operate over AC and DC high voltage lines until 1100 KV that reach data rate of hundreds of Kbps. High voltage lines are good waveguides where PLC can be used for remote fault detection and recently high voltage digital modems reached to support data rates of 320 Kbps and range of 100 Km, also signals of UNB-PLC propagate easily through low voltage transformers. A very important application of PLC is the vehicle to grid communication
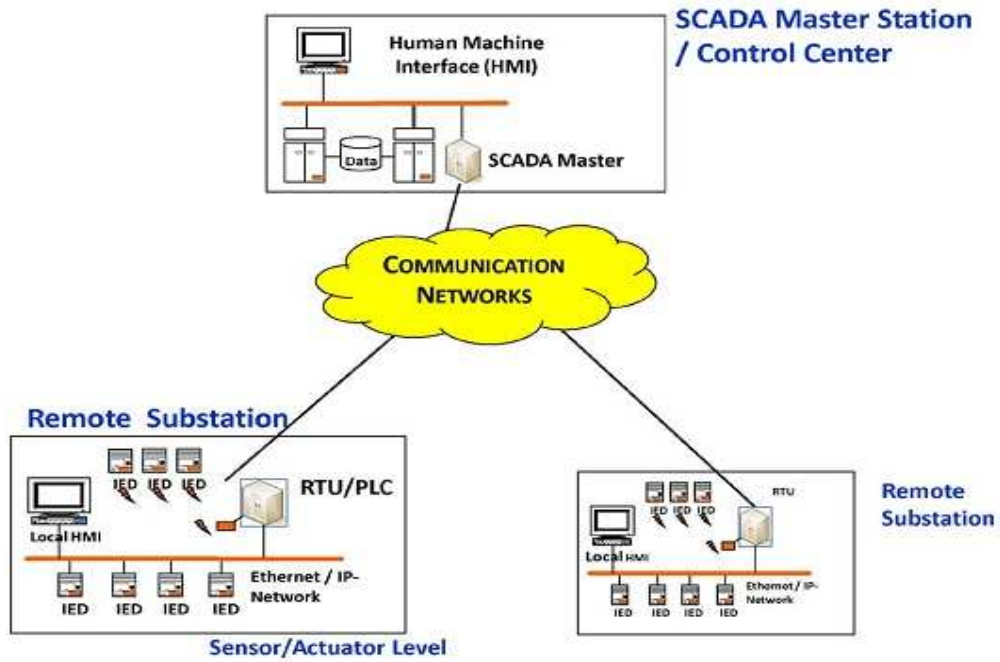
FIGURE 1.2: SCADA system in power grid [4].

where this physical association provides also high security level. The need of communication in smart grid is increasing to allow more control and interaction between different networks, so that we can face accidents of equipment failure and fluctuations of supply and demand. Communication in smart grid can be applied to Supervisory Control and Data Acquisition (SCADA) which is the model managing the power network. It is helping to optimize the power system operation and make electric supply more stable as shown in Fig. 1.2. Also communication in smart grid can be applied to Cyber physical systems control and sensing because the physical network of the power grid includes a wide area network of sensors that helps to report system failures at any time. Power Line Communication can be used in many different roles in smart grid.

1.2.1 PLC for high voltage networks

It is important to support applications of state estimation, protective relaying, remote station surveillance and power system control as shown in Fig. 1.3.
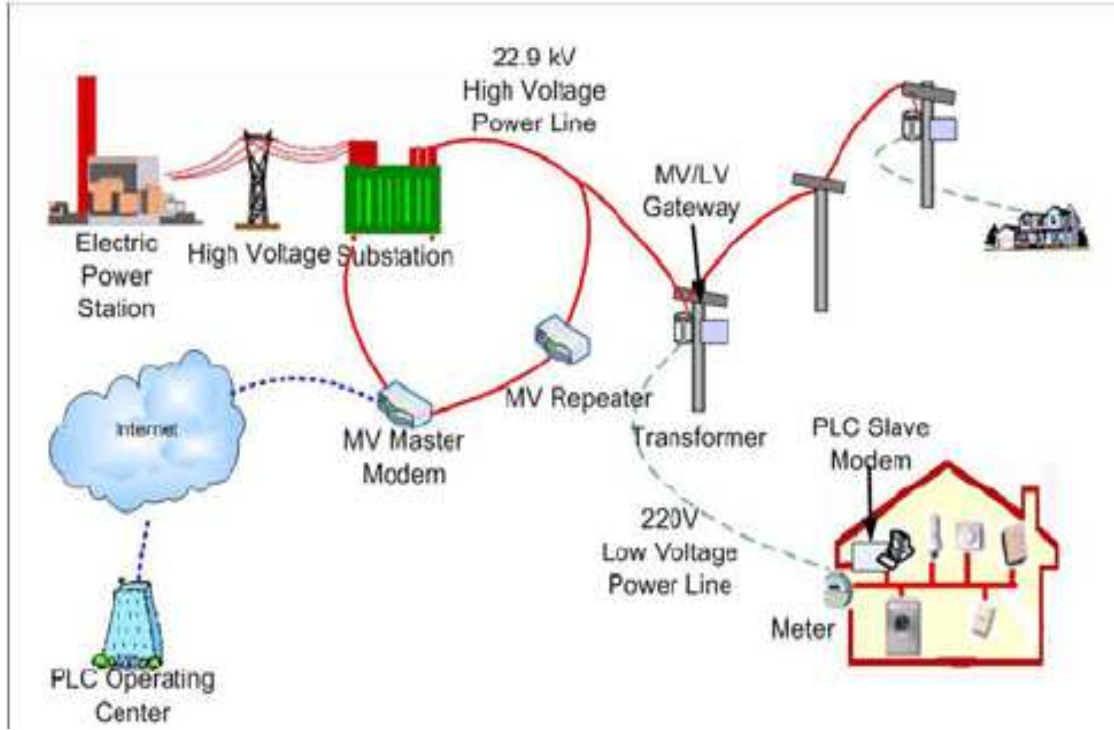
FIGURE 1.3: Overview of PLC Network Architecture with High voltage power line [5].

1.2.2 PLC for medium voltage networks

It is important to transfer information regarding the status of power flow between sub-stations. This can help to prevent islanding phenomenon and monitoring of the medium voltage site.

1.2.3 PLC for low voltage networks

Low voltage networks include the majority of PLC applications such as Automatic Meter Reading (AMR), Advanced Metering Infra-structure (AMI), vehicle-to-grid communication as shown in Fig. 1.4, Demand Side Management (DSM) and Home-Energy Management.

1.3 Thesis Contribution

In this thesis, we have
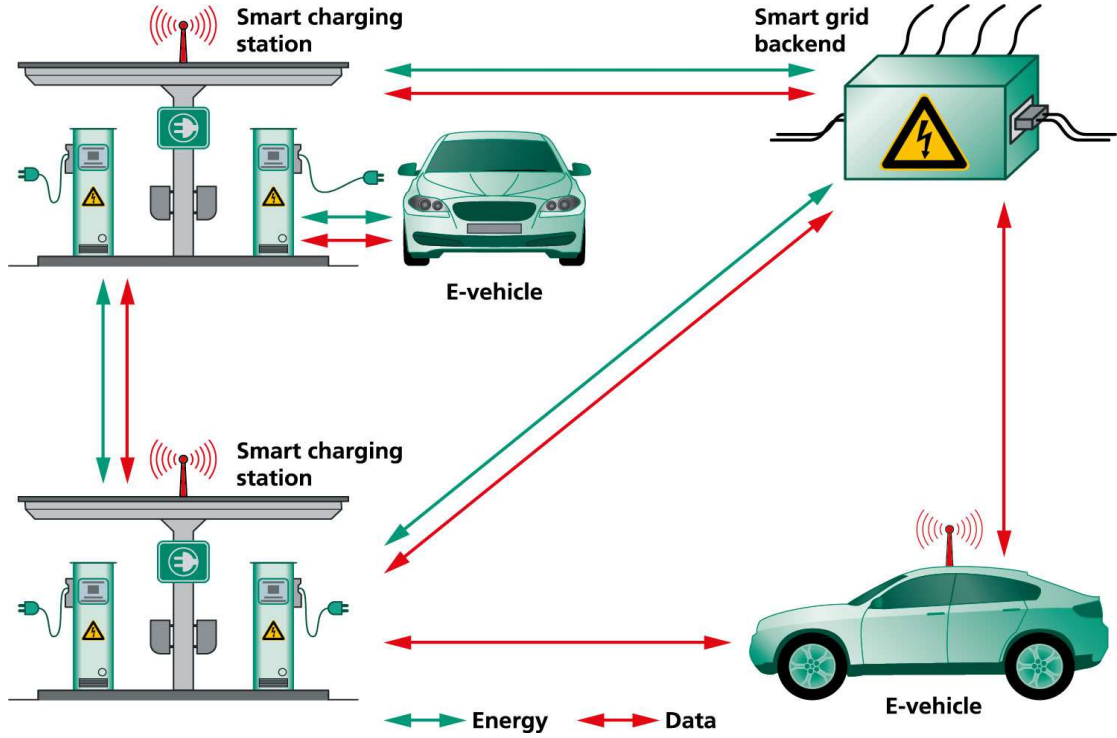
FIGURE 1.4: Information Exchange before, during and after Charging through vehicle-to-grid communication [6].

1. Presented a study of power line communications with two priority levels of data using hierarchical QAM modulation in impulsive noise with Bernoulli and Poisson arrivals.

2. Derived Closed-form expressions for the error probability for each priority level for both single carrier and OFDM in SISO and MIMO systems.

3. Developed a bit loading algorithm to provide UEP for the frequency-selective PLC channel.

4. Analyzed the performance of 4/16 QAM system in PLC cyclostationary noise.

5. Described three different MIMO architectures for use in PLC systems to allow more control over the UEP levels.

6. Extended UEP to four different levels.

7. Improved BER using joint transmit and receive Beamforming.

1.4   Thesis Organization

In chapter 2, we present a background overview of the PLC channel and noise models then we analyze the performance of UEP system in PLC cyclostationary noise. Chapter 3 constitutes the major contribution of the thesis, in which we consider the design of UEP scheme using 4/16 QAM hierarical modulation for single-carrier and OFDM systems then we present a developed bit loading algorithm to provide UEP for the frequency-selective PLC channel. Chapter 4 presents the analysis of our system over a MIMO PLC channel, extension of UEP into four different levels and applying Beamforming technique. In chapter 5, we present the thesis conclusion and some directions for future research.

Chapter 2

PLC Channel and Noise models

2.1 PLC Channel

According to [7] and [8] PLC channel is modeled by two approaches which are the multipath model and the transmission line model.

2.1.1 Multipath Model

A multipath model was proposed in [9] for power line channels based on physical effects, multipath propagation and cable losses. This multipath model consists of many parameters that need to be determined and estimated according to some training data, however it does not depend on the network topology and the frequency response is given by the following equation.

$$H(f) = \sum_{i=1}^{N} g_i \times exp^{-(a_o + a_1 f^k)d_i} \times exp^{-j2\pi f \tau_i} \qquad (2.1)$$

Where the parameters are illustrated as in Table 2.1

The disadvantages of this model is including large number of parameters that need a complex estimation process, besides not being able to determine the parameters change from site to site. Also, these parameters can be viewed as random variables across different sites and get a statistical model for the PLC channel. While its advantage is that it does not require knowing the network topology.

TABLE 2.1: Multipath model parameters

Parameter	Definition
i	path index
a_o , a_1	attenuation parameters
k	exponent of attenuation factor
g_i	weighting factor
d_i	path length
τ_i	path delay
N	number of paths

TABLE 2.2: Transmission Line model parameters

Parameter	Definition
Z_s	Transmitter port impedance
Z_L	Receiver port impedance
Z_{in}	$\dfrac{A \times Z_L + B}{C \times Z_L + D}$

2.1.2 Transmission Line Model

A transmission line model was proposed in [10] for power line channels based on the representation of transmission lines by ABCD matrices. It is based on modeling of all electrical components of the PLC network as 2-port network. Most of the electrical components have physical models and can get their ABCD parameters, also other components which lack a physical model can be characterized by vector network analyzers. The whole equivalent ABCD parameters between the transmit and receive ports are computed to get the transfer function of that link using the following equation as stated in [8].

$$H(f) = \frac{Z_{in}}{(Z_s + Z_{in})(A + \dfrac{B}{Z_L})} \tag{2.2}$$

Where the parameters are illustrated as in Table 2.2

The advantage of this model is that it does not need channel measurement for fitting parameters, also it is a deterministic model based on the knowledge of network topology and its electric components.

A generator for PLC channels was developed in [11] and the default channel of this generator was used in simulation of the system developed in this thesis.

2.2   PLC Noise

The noise in power lines can not be represented by additive white gaussian noise because it is more complicated and includes different types of noise. As stated in [12] the noise in PLC can be divided into five general classes as follows.

2.2.1   PLC Noise Classes

1. Colored background noise

   It is characterized by low power spectral density PSD which vary with frequency and it is caused by summation of noise generated from several different sources such as household appliances.

2. Narrow-band noise

   It is composed of sinusoidal signals with modulated amplitude which resulted from broadcast radio stations.

3. Asynchronous periodic impulsive noise

   It occurs with a repetition rate between 50 and 200 KHz and it is mainly caused by switched power supplies.

4. synchronous periodic impulsive noise

   It occurs with repetition rate of 50 Hz because it is synchronous with the mains frequency and it has PSD which decreases with frequency. Also, it is caused by power supplies due to the switching of rectifier diodes.

5. Asynchronous impulsive noise

   These impulses are characterized by random duration and random occurrence where it is caused by switching transients in the network. This kind of impulses has high energy and their PSD can reach values of more than 50 dB above the background noise that may cause burst errors in data transmission.

According to [13], asynchronous impulsive noise is the dominant component in broadband PLC and synchronous periodic impulsive noise is the dominant component in narrowband PLC; where each of them is explained in more details as follows.

2.2.2 Asynchronous Impulsive Noise

It is the dominant component in broadband PLC and it can be described by three random variables which are amplitude, impulse width and inter-arrival time [14]. [12] presented a statistical model of this impulse noise describing its amplitude, impulse width and inter-arrival time because this type of noise is considered a critical problem that may degrade high speed communication causing burst errors. The disturbance ratio, which is the percentage of total impulse time to an observation window, is less than 1%; however PLC systems should use error detection and correction schemes to avoid this kind of noise and to improve the communication system performance in power lines.

2.2.3 Synchronous Periodic Impulsive Noise

It is the dominant component in narrowband PLC and it contains larger noise bursts than asynchronous impulsive noise that may corrupt many consecutive symbols. Two of the models developed to represent this class of noise are presented as follows.

2.2.3.1 The Cyclostaionary Model Presented by M. Katayama

In [15] a model was presented to describe this class of noise and considered it to be cyclostationary additive Gaussian noise with zero mean and the variance is synchronous to the mains voltage, where the noise pdf was given by :

$$P(n(iT_s)) = \frac{1}{\sqrt{2\pi\sigma^2(iT_s)}} exp^{\dfrac{-n^2(iT_s)}{2\sigma^2(iT_s)}} \qquad (2.3)$$

Where $\sigma^2(iT_s)$ is the variance which is periodic with frequency equals half the mains frequency. This variance function was approximated by a simple function with a small
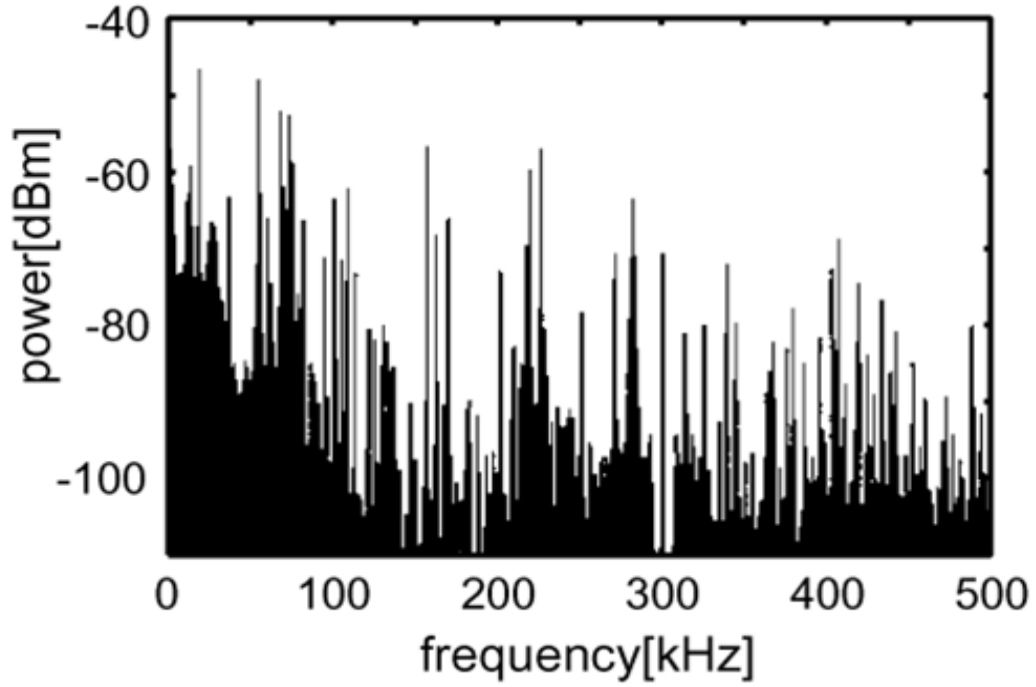
FIGURE 2.1: The non-white noise in power lines shown in [15].

number of parameters given by :

$$\sigma^2(iT_s) = \sum_{l=0}^{L-1} A_l |\sin(\frac{2\pi t}{T_{AC}} + \theta_l)|^{n_l} \tag{2.4}$$

Where it contain 3L parameters A_l, θ_l and n_l that need to be estimated.

Since the noise in power lines is non-white as shown in Fig. 2.1, the variance is multiplied by a decaying exponential term taking into account that the noise power is a time function.

$$\sigma^2(t,f) = \sigma^2(t) \times \frac{a}{2} exp^{-a|f|} \tag{2.5}$$

After the process of parameters estimation the variance is modeled as shown in Fig. 2.2.

The generation of noise waveform as in Fig. 2.3 is completed after generation of gaussian noise with the variance derived and passing it to filter with frequency response as in eq.(2.5).

Katayama noise model was simulated during this thesis work and the simulation results are shown in Fig. 2.4, Fig. 2.5, Fig. 2.6, Fig. 2.7 and Fig. 2.8.
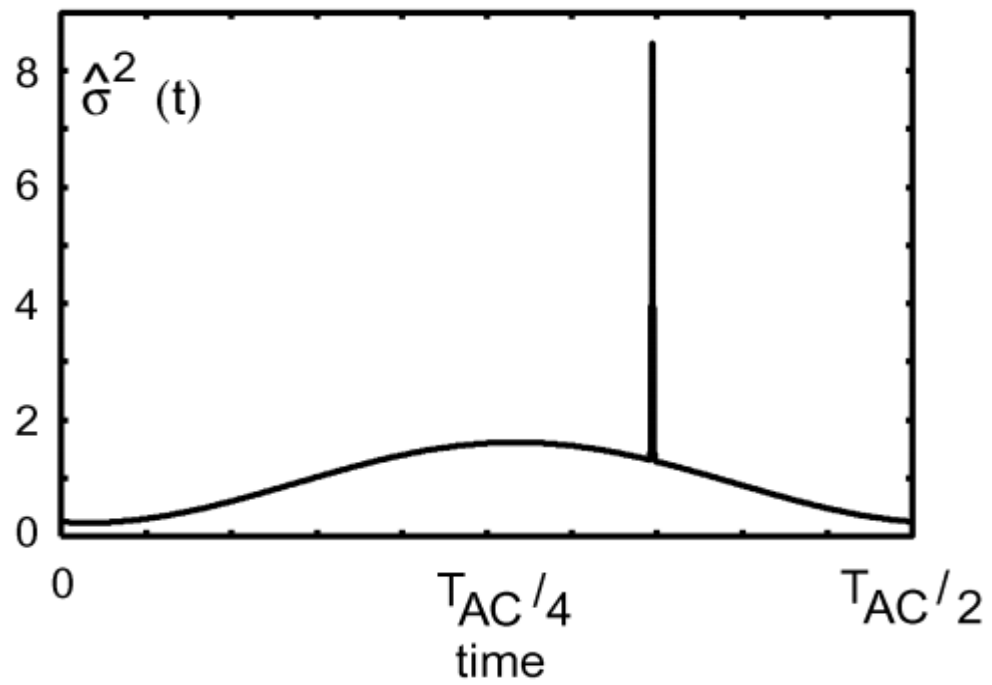
FIGURE 2.2: The variance of PLC noise shown in [15].

FIGURE 2.3: The generation of PLC noise waveform shown in [15].
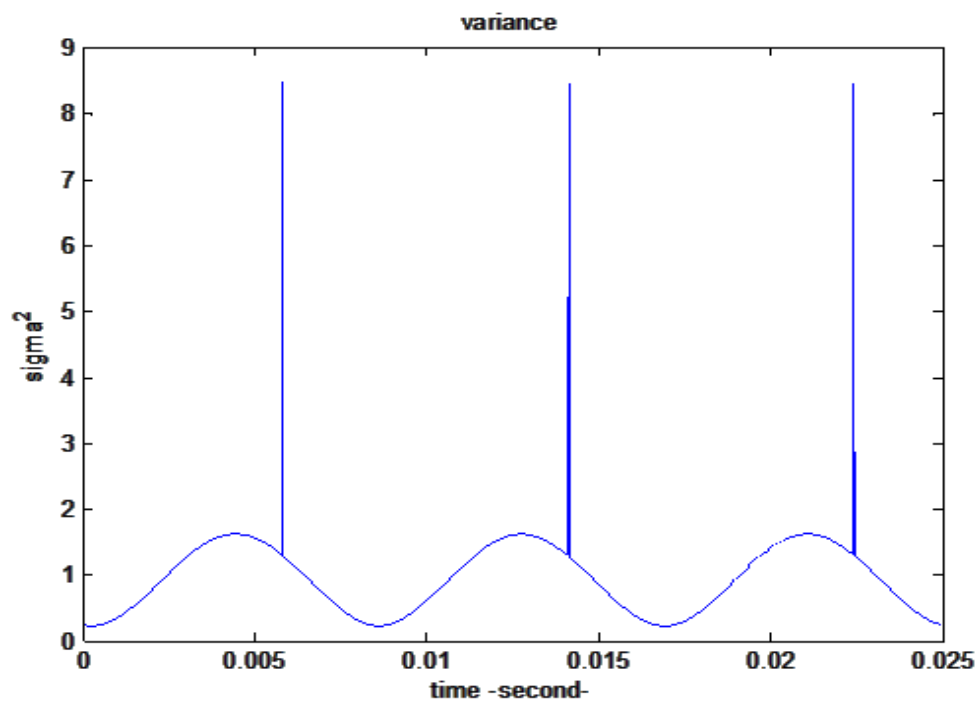
FIGURE 2.4: Our simulation result for the variance of PLC noise shown in [15].

FIGURE 2.5: Our simulation result for the colored noise spectrum of PLC noise shown in [15].
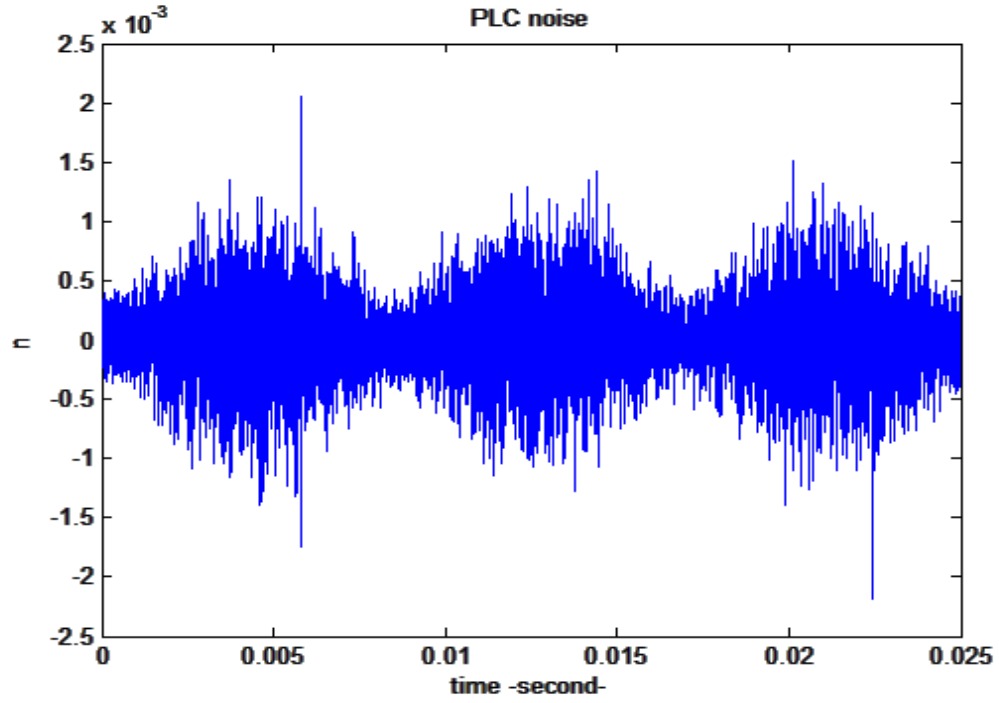
FIGURE 2.6: Our simulation result for the generation of PLC noise shown in [15].

2.2.3.2 The Cyclostaionary Model Presented by M. Nassar

In [16] another model was presented to describe the synchronous periodic impulsive noise in power lines, that model was based on the generation of cyclostationary noise as a result of sequential filtering of stationary input by a sequence of linear time invariant LTI filters as shown in Fig. 2.7. So the noise is modeled as the response of linear periodically time-varying LPTV system to a stationary input to result in the PLC noise shown in Fig. 2.8.

Nassar noise model was simulated during this thesis work as shown in Fig. 2.9 where this periodic noise can be divided into three main regions. The first region $(0-5ms)$ corresponds to low power background noise region, the second region $(5-7ms)$ corresponds to high power interference and the third region $(7-7.3ms)$ corresponds to broadband impulse. The performance of a hierarchical 4/16 QAM system was investigated using this noise model as shown in Fig. 2.10 where the simulated BER with PLC noise model is compared with the theoretical BER regarding this noise as an additive gaussian noise with three different variances.
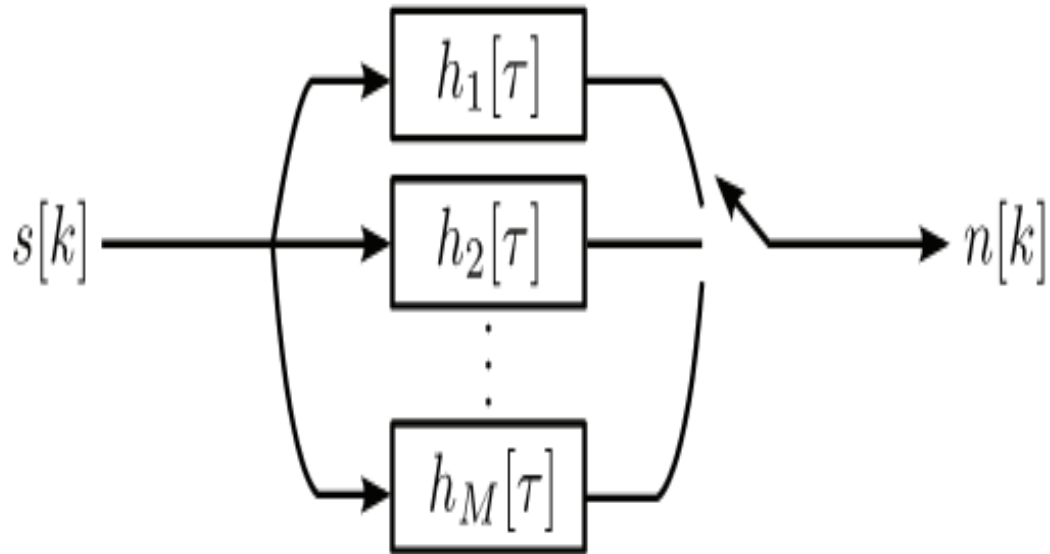
FIGURE 2.7: LTI filters for generation of the PLC noise model shown in [16].
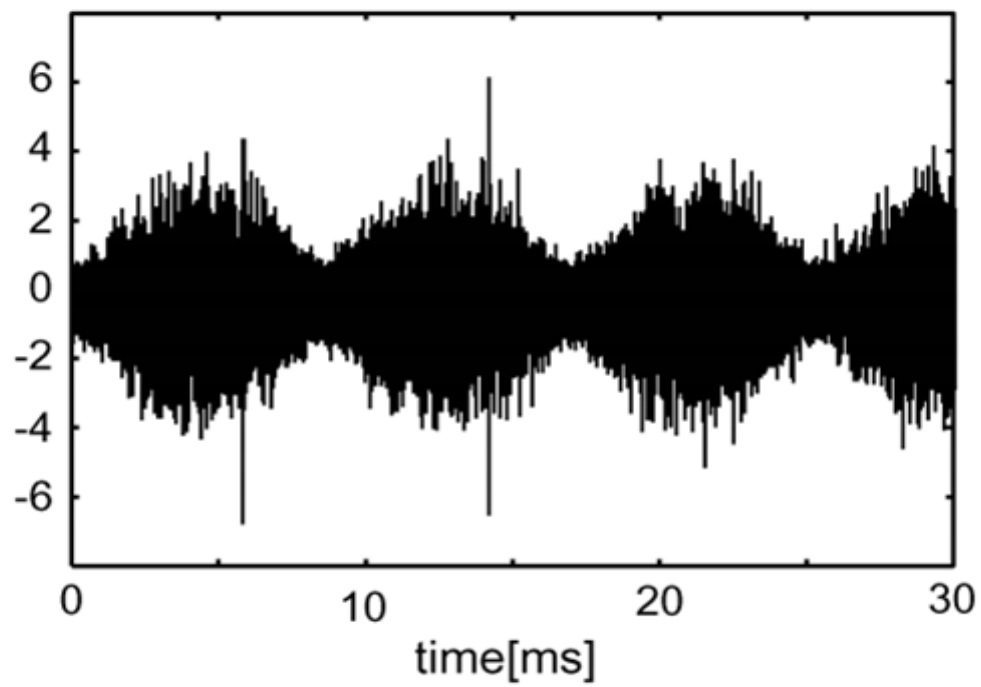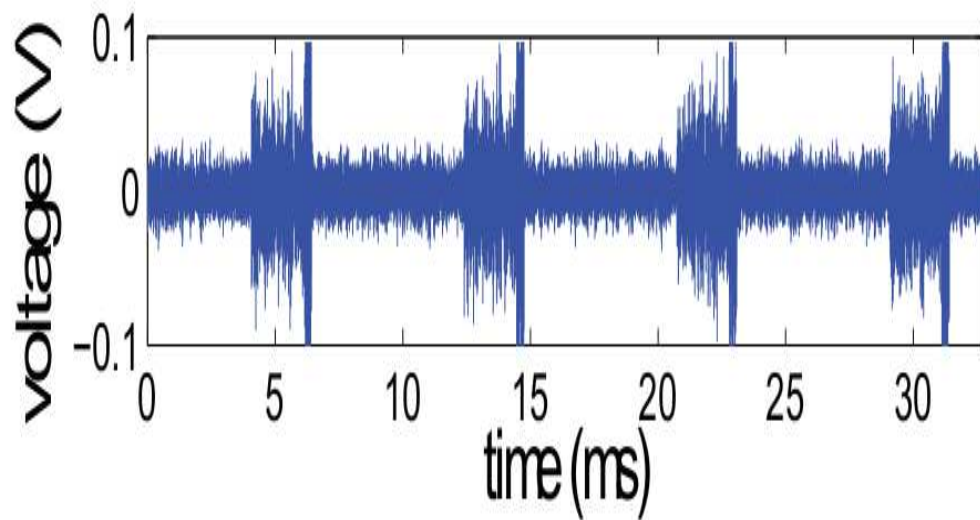

FIGURE 2.8: The generation of PLC noise waveform shown in [16].

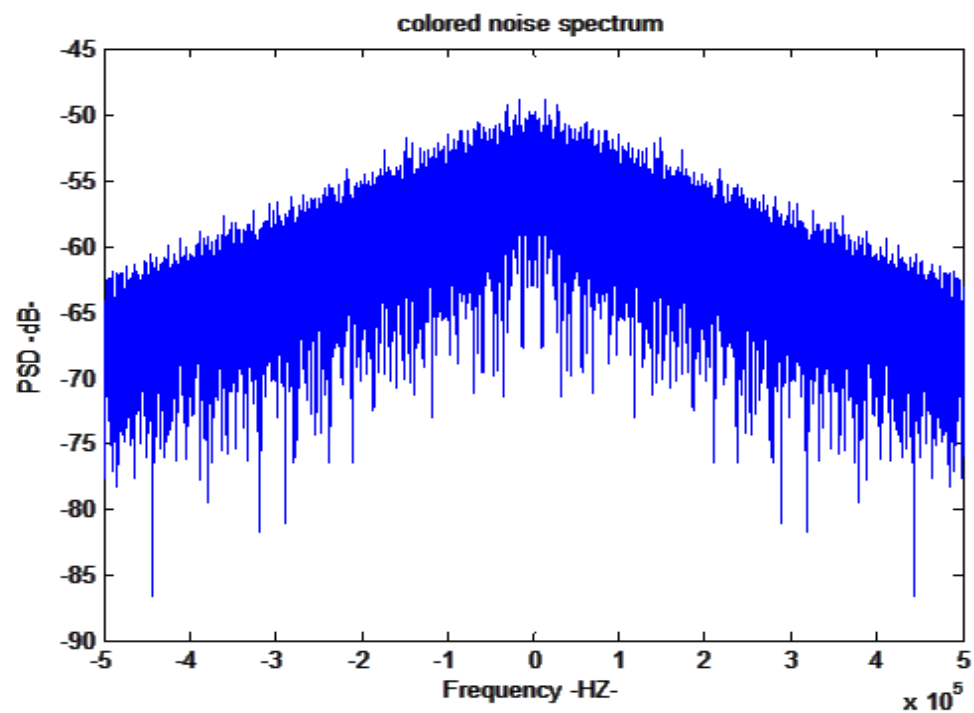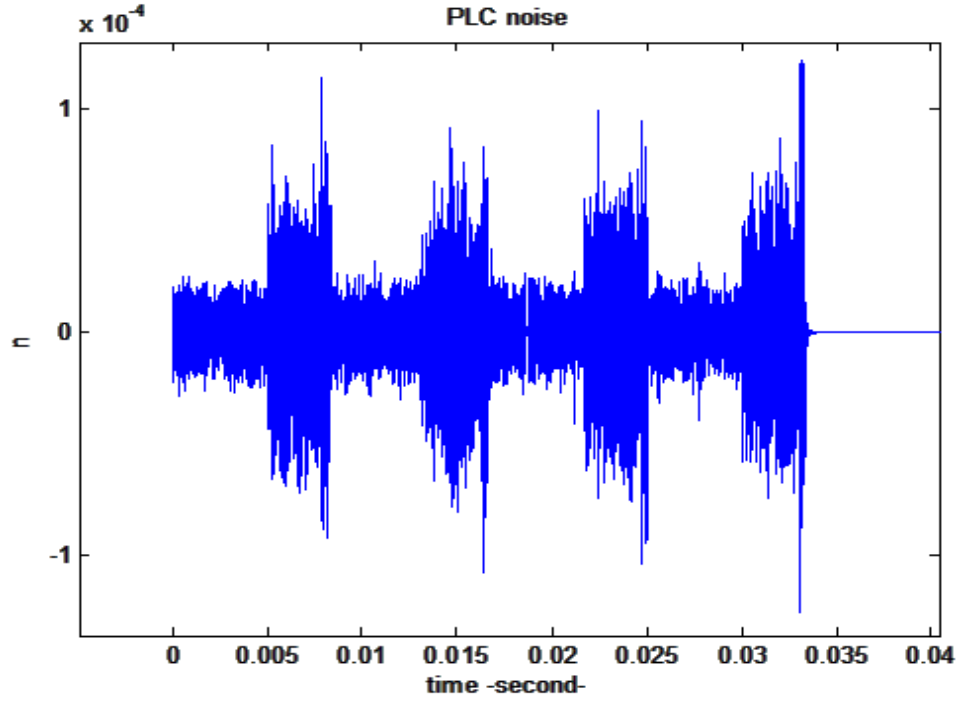FIGURE 2.9: Our simulation result for the generation of PLC noise shown in [16].
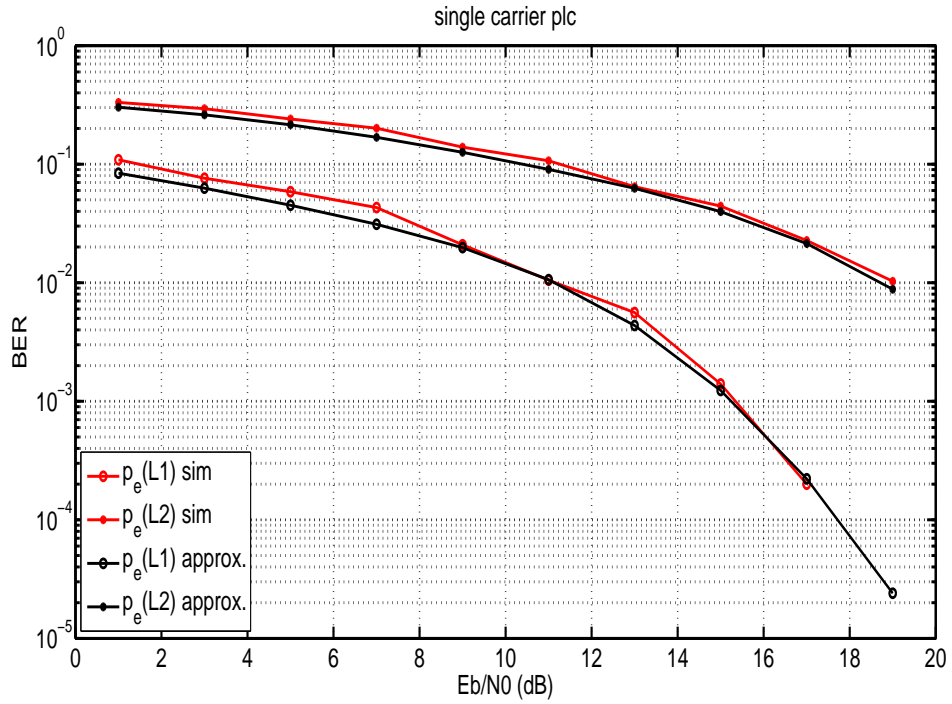
FIGURE 2.10: Our simulation result for hierarchical 4/16 QAM single carrier system within the PLC noise model described in [16].

Chapter 3

Unequal Error Protection in PLC Channel

3.1   Introduction

The main problem with PLC is its noise which is not the simple AWGN model [17]. A lot of work has been done to model the noise over power lines. This can be divided into narrow-band PLC noise models, e.g. [15, 16], and wide-band PLC noise models, e.g. [12]. Broadband PLC with impulsive noise was studied in [18] but for a single priority level of data. On the other hand, little work has been done on unequal error protection (UEP) techniques for PLC, e.g. [19], which considered a different noise model from our model, and focused on video transmission. In [20], UEP was implemented through LDPC codes. In this work, we consider the problem of UEP over impulsive noise channels for PLC. Closed-form expressions for the error probability are derived for hierarchical 4/16 QAM system in impulsive noise for single carrier and OFDM cases. Based on those, a bit loading algorithm is developed to provide UEP for this PLC system. Improvement due to our bit loading algorithm is demonstrated. Analytical results are presented together with simulations.

3.2   PLC Channel and Hierarical Modulation

According to [18] the noise in PLC channels has two components; the first one is the background noise which is modeled as AWGN with zero mean and variance N_o. The second one is impulsive noise that has a Gaussian pdf with zero mean and variance N_i and the impulsive noise arrivals are modeled by a Poisson arrival process. For simplicity, the analysis is first carried out assuming Bernoulli arrivals, and then the analysis is extended to the Poisson arrival model.

The additive noise at the output of the receiver matched filer may be expressed as follows

$$n_{\text{total}} = n_{\text{background}} + n_{\text{impulsive}}, \tag{3.1}$$

where $n_{\text{background}}$ is the background AWGN and $n_{\text{impulsive}}$ is the impulsive noise component. For the Bernoulli arrival model:

$$n_{\text{impulsive}} = \frac{T_{\text{impulse}}}{T_{\text{symbol}}} \times b \times n, \tag{3.2}$$

where $\frac{T_{\text{impulse}}}{T_{\text{symbol}}}$ is the ratio between impulse width and symbol duration, b is a Bernoulli random variable with probability p and n is a Gaussian random variable with zero mean and variance N_i.

For the Poisson arrival model, the noise for an arrival is given by

$$n_{\text{impulsive}} = \frac{T_{\text{impulse}}}{T_{\text{symbol}}} \times K \times n, \tag{3.3}$$

and K is a Poisson random variable with rate λ impulses per second that denotes the number of arrivals in one symbol duration.

In [11], a model was developed for channel generation based on the power lines network and loads. This model was developed for broadband indoor power line channels. In our work, we use the channel model for the PLC channel of [11], which is based on certain network parameters and load parameters given in [11]. This model generates a channel with the squared magnitude response shown in Fig. 3.1.

In this work, two levels of data protection are achieved using hierarchical QAM constellation consisting of 4-QAM embedded in 16-QAM. As shown in Fig. 3.2, the first
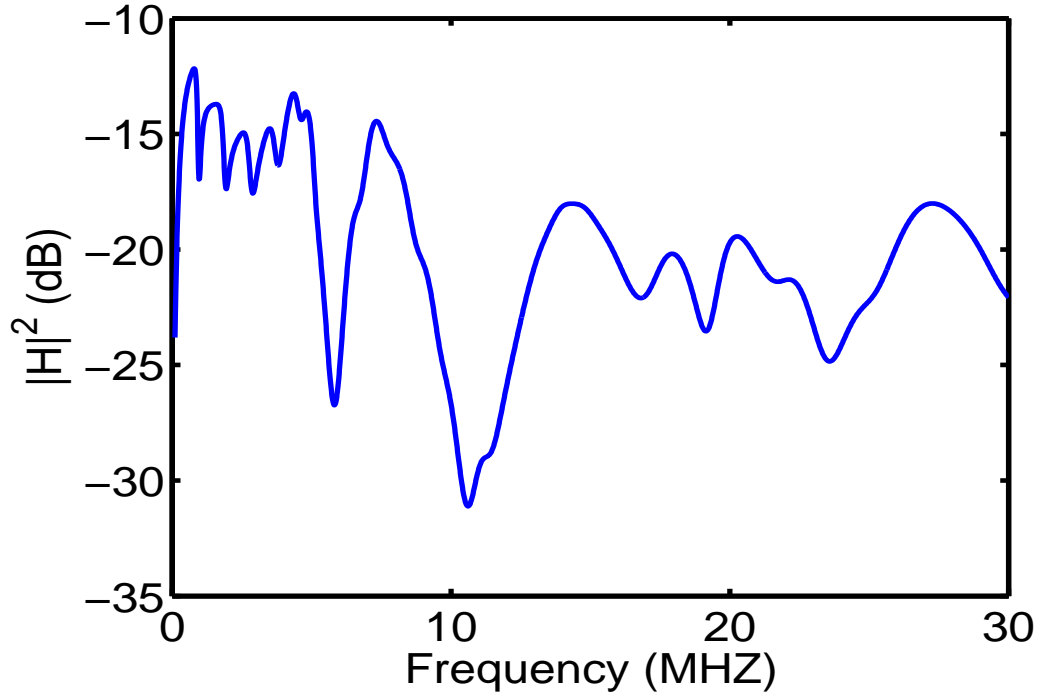
FIGURE 3.1: The default best case PLC channel as given in [11].

and second bits are more protected than the third and fourth bits where d_1 determines the protection for the higher priority level and d_2 determines the protection for the lower priority level. Note that the 4-QAM constellations are rotated across quadrants to maintain overall Gray encoding for the larger 16-QAM constellation.

3.3 System Analysis

In [21], the BER analysis for the constellation shown in Fig. 3.2 over AWGN channels was presented. In this section, we apply this analysis to the case of impulsive noise with Bernoulli and Poisson arrivals.

The BER for the more protected level ($L1$) over AWGN is given by [21]

$$p_e(L1) = \frac{1}{4}\textbf{erfc}\left(\frac{d_1 - d_2}{\sqrt{N_o}}\right) + \frac{1}{4}\textbf{erfc}\left(\frac{d_1 + d_2}{\sqrt{N_o}}\right) \tag{3.4}$$

which may be approximated, by retaining only the dominant terms, as

$$p_e(L1) \approx \frac{1}{4}\textbf{erfc}\left(\frac{d_1 - d_2}{\sqrt{N_o}}\right) \tag{3.5}$$

FIGURE 3.2: 4/16 QAM constellation.

The BER for the less protected level ($L2$) over AWGN is given by

$$p_e(L2) = \frac{1}{2}\mathbf{erfc}\left(\frac{d_2}{\sqrt{N_o}}\right) - \frac{1}{4}\mathbf{erfc}\left(\frac{2d_1 + d_2}{\sqrt{N_o}}\right)$$
$$+ \frac{1}{4}\mathbf{erfc}\left(\frac{2d_1 - d_2}{\sqrt{N_o}}\right) \quad (3.6)$$

which can likewise be approximated as

$$p_e(L2) \approx \frac{1}{2}\mathbf{erfc}\left(\frac{d_2}{\sqrt{N_o}}\right) \quad (3.7)$$

where again N_o is the complex noise variance for the AWGN. The objective of the approximations is to simplify the calculation of constellation distances in the bit loading algorithm to be presented in the sequel, with very high accuracy. Next, we derive the BER expressions over impulsive noise PLC channels for the single carrier and OFDM systems.

3.3.1 Single Carrier Analysis

For Bernoulli arrivals, the received symbol will suffer from noise with two different variances. The noise variance will be N_o when no impulsive noise arrival occurs and $N_o + N_i$ in the case of impulsive noise arrival; note that the noise will be Gaussian in both cases. The underlying assumption is that the probability of two or more impulses within a symbol may be neglected. The approximated BER for impulsive noise with Bernoulli arrivals may be expressed as (averaging over the two noise variances probabilities)

$$p_e(L1) \approx (1-p) \times \frac{1}{4}\mathbf{erfc}\left(\frac{d_1 - d_2}{\sqrt{N_o}}\right)$$
$$+ p \times \frac{1}{4}\mathbf{erfc}\left(\frac{d_1 - d_2}{\sqrt{N_o + N_i}}\right) \tag{3.8}$$

$$p_e(L2) \approx (1-p) \times \frac{1}{2}\mathbf{erfc}\left(\frac{d_2}{\sqrt{N_o}}\right)$$
$$+ p \times \frac{1}{2}\mathbf{erfc}\left(\frac{d_2}{\sqrt{N_o + N_i}}\right). \tag{3.9}$$

For the case when the probability of two or more impulses within a symbol is non-negligible, a Poisson arrival model is more appropriate. The approximate conditional BER for impulsive noise with Poisson arrivals, conditioned on k arrivals within a symbol duration, may be expressed as

$$p_e(L1|k \ impulse \ arrivals) \approx \frac{1}{4}\mathbf{erfc}\left(\frac{d_1 - d_2}{\sqrt{N_o + kN_i}}\right) \tag{3.10}$$

Averaging over the Poisson random variable K

$$p_e(L1) = E_K[p_e(L1|k \text{ impulse arrivals})] \tag{3.11}$$

$$p_e(L1) \approx \sum_{k=0}^{\infty} \frac{1}{4}\mathbf{erfc}\left(\frac{d_1 - d_2}{\sqrt{N_o + kN_i}}\right) e^{-\alpha}\frac{\alpha^k}{k!} \tag{3.12}$$

where $\alpha = \lambda T_{\text{symbol}}$

Similarly,

$$p_e(L2) \approx \sum_{k=0}^{\infty} \frac{1}{4}\mathbf{erfc}\left(\frac{d_2}{\sqrt{N_o + kN_i}}\right) e^{-\alpha}\frac{\alpha^k}{k!} \tag{3.13}$$

3.3.2   OFDM Analysis

In an OFDM based system, the first stage in the receiver is the DFT block. The time domain impulsive noise is spread in the frequency domain after the receiver DFT, so the impulse effect is spread equally over all used subcarriers. Therefore, in the case of OFDM systems, all the subcarriers will experience the same noise variance. The total noise PSD will be flat and equals the sum of the background noise variance, N_o, and the impulse noise variance (which depends on the number of impulsive noise arrivals in an OFDM symbol).

For the case of Bernoulli arrivals, the number of impulses in the time domain will have a binomial distribution. The underlying assumption here is that no more than M impulses will arrive within an OFDM symbol. For correspondence with the single-carrier case, this means no more than one impulse arrives during $T_{\text{OFDM Sym}}/M$ where $T_{\text{OFDM Sym}}$ is the OFDM symbol duration and M is the number of subcarriers in the OFDM symbol. Hence, the BER for impulsive noise with Bernoulli arrivals may be expressed as

$$p_e(L1) \approx \sum_{k=0}^{M} \binom{M}{k} p^k (1-p)^{M-k} \times \frac{1}{4}\mathbf{erfc}\left(\frac{d_1 - d_2}{\sqrt{N_o + kN_i}}\right) \tag{3.14}$$

$$p_e(L2) \approx \sum_{k=0}^{M} \binom{M}{k} p^k (1-p)^{M-k} \times \frac{1}{2}\mathbf{erfc}\left(\frac{d_2}{\sqrt{N_o + kN_i}}\right) \tag{3.15}$$

The approximate conditional BER for impulsive noise with Poisson arrivals, conditioned on k arrivals within an OFDM symbol duration, may be expressed as

$$p_e(L1|k \ impulse \ arrivals) \approx \frac{1}{4}\mathbf{erfc}\left(\frac{d_1 - d_2}{\sqrt{N_o + kN_i}}\right) \tag{3.16}$$

Averaging over the Poisson random variable K

$$p_e(L1) = E_K[p_e(L1|k \ \text{impulse arrivals})] \tag{3.17}$$

$$p_e(L1) \approx \sum_{k=0}^{\infty} \frac{1}{4}\mathbf{erfc}\left(\frac{d_1 - d_2}{\sqrt{N_o + kN_i}}\right) e^{-\alpha_o} \frac{\alpha_o^k}{k!} \tag{3.18}$$

where $\alpha_o = \lambda T_{\text{OFDM Sym}}$. Note that OFDM has the effect of increasing the symbol duration so the expected number of noise impulses per symbol increases.

Similarly,

$$p_e(L2) \approx \sum_{k=0}^{\infty} \frac{1}{4}\mathbf{erfc}\left(\frac{d_2}{\sqrt{N_o + kN_i}}\right) e^{-\alpha_o}\frac{\alpha_o^k}{k!} \tag{3.19}$$

Note that the BER expressions derived above are impractical for use in the bit loading algorithm to be presented later. Therefore, we adopt approximate BER expressions that provide good approximations for the BER and simplify the bit loading algorithm. The approximation is based on modeling the noise as AWGN whose variance equals the average variance of the total noise (where the total noise includes the background noise and the impulsive noise). The BER for impulsive noise with Bernoulli arrivals may be expressed as

$$p_e(L1) \approx \frac{1}{4}\mathbf{erfc}\left(\frac{d_1 - d_2}{\sqrt{N_t}}\right) \tag{3.20}$$

$$p_e(L2) \approx \frac{1}{2}\mathbf{erfc}\left(\frac{d_2}{\sqrt{N_t}}\right) \tag{3.21}$$

where $N_t = N_o + p \times M \times N_i$.

The BER for impulsive noise with Poisson arrivals may be expressed as

$$p_e(L1) \approx \frac{1}{4}\mathbf{erfc}\left(\frac{d_1 - d_2}{\sqrt{N_t}}\right) \tag{3.22}$$

$$p_e(L2) \approx \frac{1}{2}\mathbf{erfc}\left(\frac{d_2}{\sqrt{N_t}}\right) \tag{3.23}$$

where $N_t = N_o + \sum_{k=0}^{\infty} kN_i e^{-\alpha_o}\frac{\alpha_o^k}{k!}$. It was found that the above variance may be computed accurately using the first 1000 terms of the summation. This computation is performed offline.

3.4 Bit Loading

We now describe our proposed bit loading algorithm which is based on the one developed in [22]; the latter being based on Hughes-Hartogs algorithm [23]. This algorithm is useful for power limited systems although it was simulated here with no power constraint and assuming perfect channel knowledge at the transmitter and the receiver. In [22], the calculation of the power increments was based on approximate equations as in [24]. However, our algorithm is based on the calculation of the power increments for each

TABLE 3.1: Input parameters for the bit loading algorithm

Parameter	Definition
N	number of subcarriers
h	channel gain
B	number of bits that can be allocated / subcarrier
$p_e(L1), p_e(L2)$	BER targeted for each priority level
$B1, B2$	bit rate targeted for each priority level
E_{target}	total power constraint

subcarrier using the derived BER equations. The algorithm is illustrated in the following steps and uses the inputs defined in Table 3.1.

Our algorithm works as follows:

- Calculate the power increment for each subcarrier m to be loaded with t more bits and $t = 2$ because our system is either sending 4-QAM or 16-QAM.

- Load the data with higher priority first. The power increment during this step is calculated as follows:

$$\Delta p_m = \frac{1}{|h_m|^2} \times 2N_t \times (\mathbf{erfc}^{-1}(2 \times p_e(L1)))^2 \tag{3.24}$$

where h_m is the channel attenuation on the m-th subcarrier.

- If the bit rate for the higher priority level is achieved and there is still power budget, bit loading is continued for the lower priority level and the power increment is calculated as follows:

$$\begin{aligned} p_{m_{new}} = \frac{1}{|h_m|^2} &\times 2N_t \times (\mathbf{erfc}^{-1}(4 \times p_e(L1)))^2 \\ &+ 4N_t \times (\mathbf{erfc}^{-1}(2 \times p_e(L2)))^2 \\ &+ 4N_t \times (\mathbf{erfc}^{-1}(2 \times p_e(L2))) \times (\mathbf{erfc}^{-1}(4 \times p_e(L1))) \end{aligned} \tag{3.25}$$

$$p_{m_{old}} = \frac{1}{|h_m|^2} \times 2N_t \times (\mathbf{erfc}^{-1}(2 \times p_e(L1)))^2 \tag{3.26}$$

$$\Delta p_m = p_{m_{new}} - p_{m_{old}} \tag{3.27}$$

- The bits are allocated to the subcarrier that gives the less power increment.

TABLE 3.2: Values of the parameters used in our first simulation

| Parameter	value
$T_{impulse}/T_{symbol}$	1
p	0.3
λ	1
N_i/N_o	1 ,10
number of subcarriers	1024

- The algorithm stops if the targeted bit rates were achieved or if there is no more power budget.

Different sub-carriers are assigned symbols with different constellation parameters so it is convenient for the receiver to run the same bit-loading algorithm used by the transmitter, so that the demodulater has same knowledge of the modulation parameters for each sub-carrier. The criterion of this modified bit-loading algorithm is to achieve the required BER for each priority level based on the derived equations for BER over impulsive noise in PLC channel while bits are allocated to the subcarrier that gives the less power increment, thus minimizing total power.

3.5 Simulation Results

First, the system is simulated without the PLC channel and with impulsive noise. All Simulations are done using **MATLAB** The two levels of data protection may be attained using hierarchical constellation parameters d_1 and d_2, as well as by setting $d_1 = 2d_2$, which represents the uniform 16-QAM constellation, and appropriate bit encoding. In the following, i.e. without PLC channel, we use a uniform QAM constellation to demonstrate the accuracy of the approximate BER expressions. We also compare single- and multi-carrier performance. The value of each parameter is given in Table 3.2.

Simulation results are plotted with the derived theoretical expressions in the following figures. The results for single carrier system in impulsive noise with Bernoulli and Poisson arrivals are shown in Fig. 3.3 and Fig. 3.4, respectively. The results for OFDM system in impulsive noise with Bernoulli and Poisson arrivals are shown in Fig. 3.5 and Fig. 3.6, respectively. The level of data protection can be further controlled by determining the constellation points separations. We assume that the PLC channel
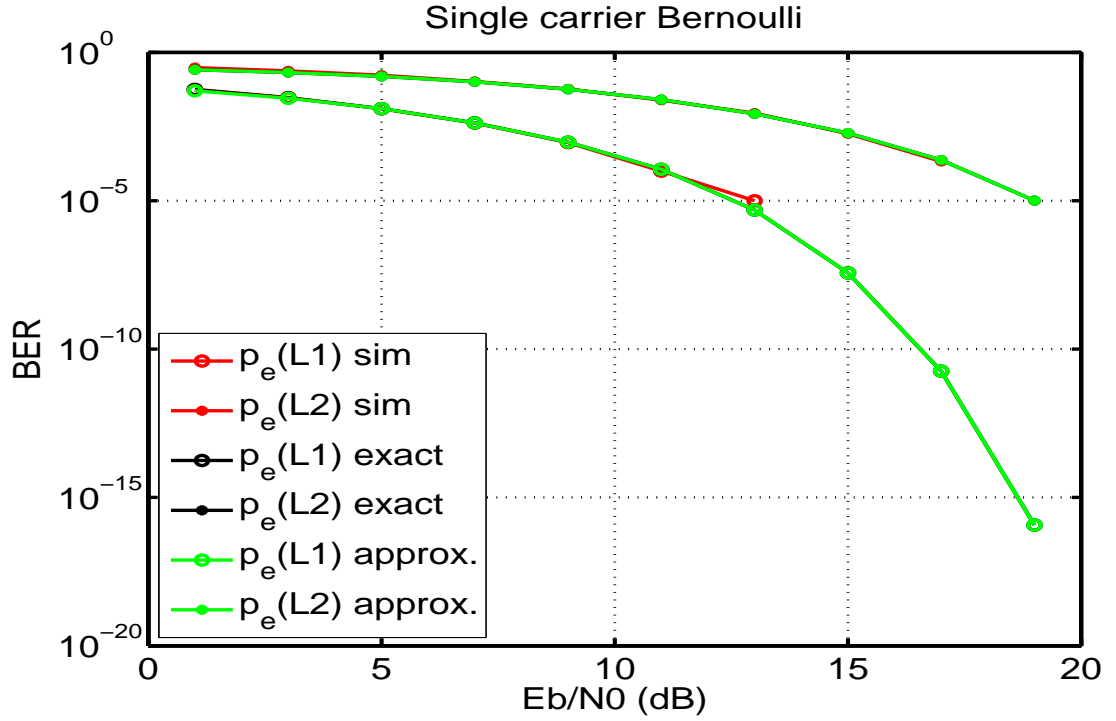
FIGURE 3.3: Single carrier with Bernoulli impulsive noise $N_i/N_o = 1$.

length is shorter than the cyclic prefix length and if this was not satisfied then a channel shortening equalizer CSE is used [25] [26] [27]. We assume sending OFDM symbol over a carrier. This OFDM simulation was done using 64 sub-carries however the proposed bit-loading algorithm has no limitation over the number of subcarriers used, so the transceiver design can support 4096 OFDM sub-carriers based on the IEEE 1901 PHY layer model [28]. Comparison between single carrier and OFDM is shown in Fig. 3.7 and Fig. 3.8. As shown in Fig. 3.7 and at strong impulsive noise, OFDM is better than single carrier at high SNR values because the effect of the impulsive noise is averaged in the OFDM case over all subcarriers. For single carrier and at low SNRs, however, the power of the noise impulses is exhausted in one or a small number of symbols. The comparison is made for the type of noise encountered in PLC, which is impulsive noise not AWGN noise, and we found OFDM to be better for part of the SNR range. For convenience we did not assume a channel in those simulations. In the practical case when there is a channel, then the well-known advantage of OFDM which is the elimination of the expensive equalizer block applies. There was no suggestion of claiming perfect equalization for the single carrier case; just that there was no channel.

Second, the system is simulated with the PLC channel model and impulsive noise using
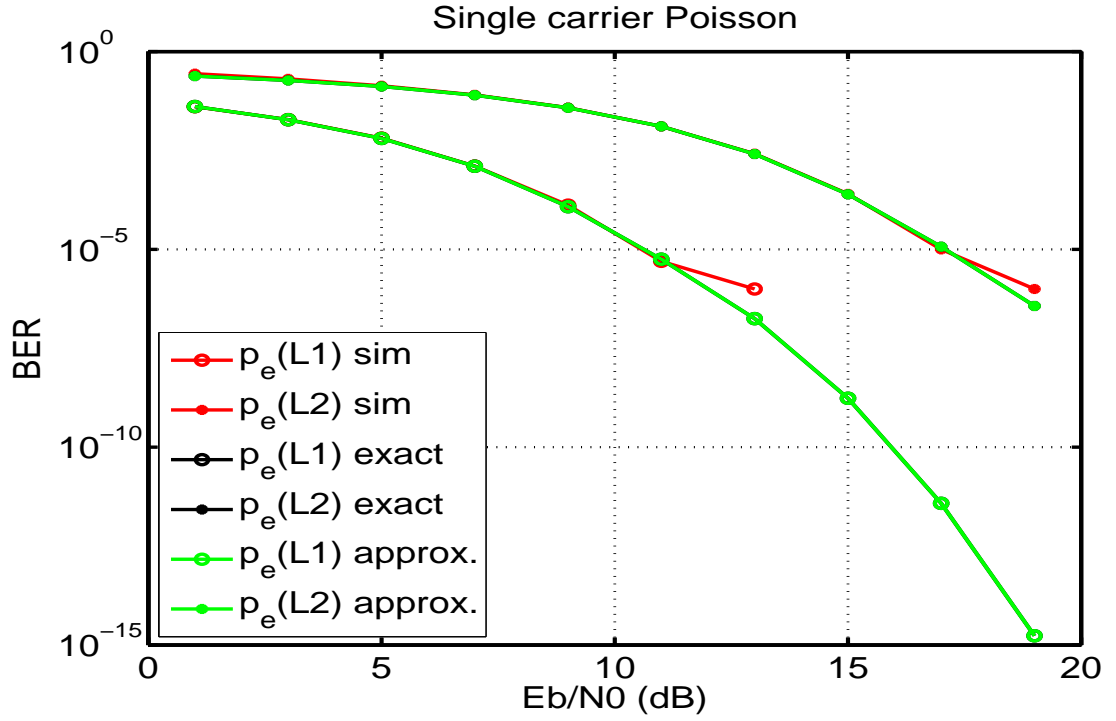
FIGURE 3.4: Single carrier with Poisson impulsive noise $N_i/N_o = 1$.
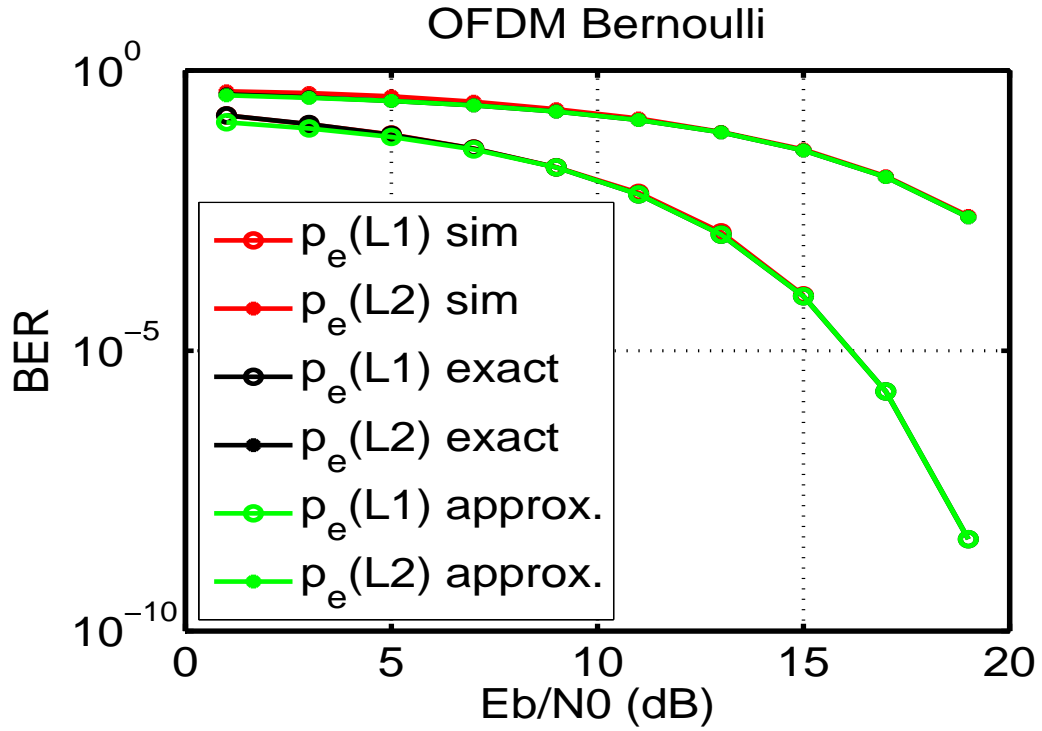
FIGURE 3.5: OFDM with Bernoulli impulsive noise $N_i/N_o = 10$.
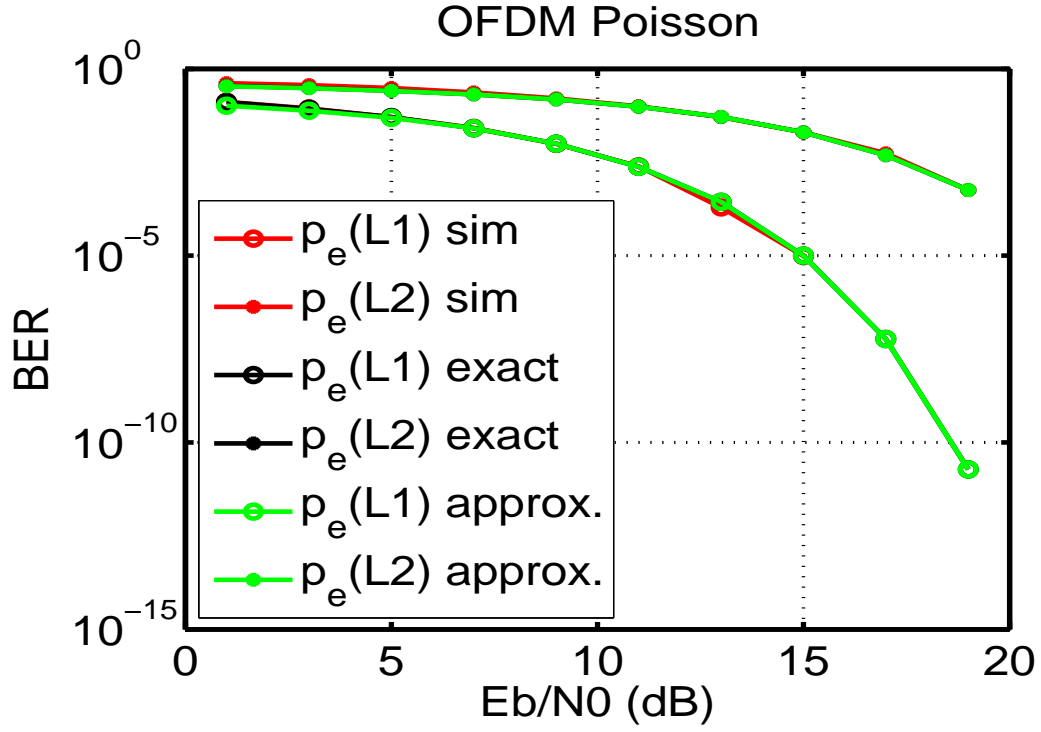
FIGURE 3.6: OFDM with Poisson impulsive noise $N_i/N_o = 1$.
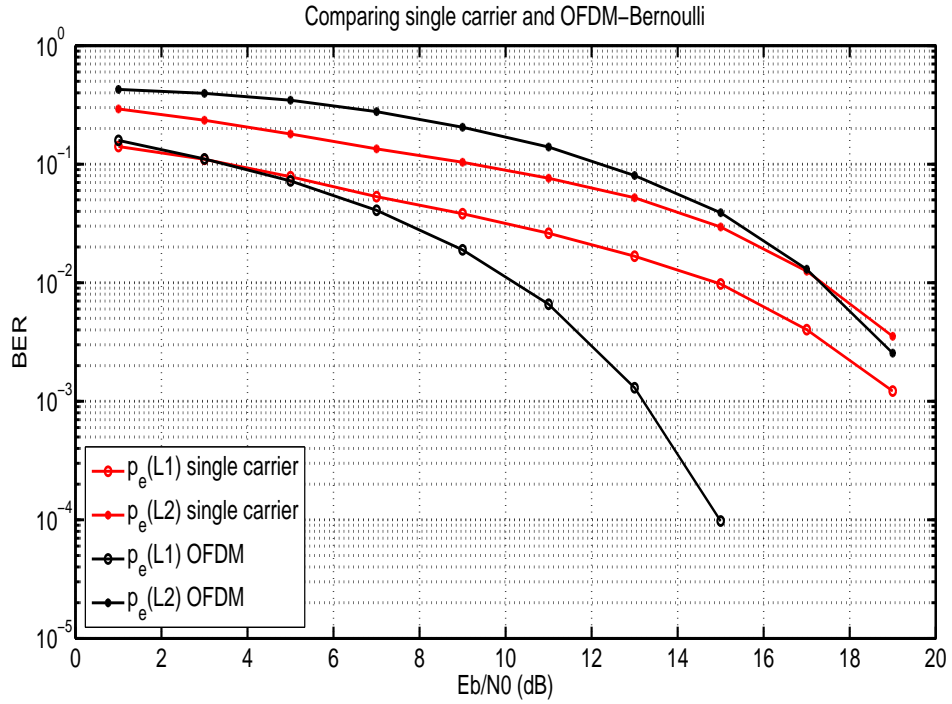
FIGURE 3.7: Comparing single carrier and OFDM at Bernoulli impulsive noise $N_i/N_o = 10$.
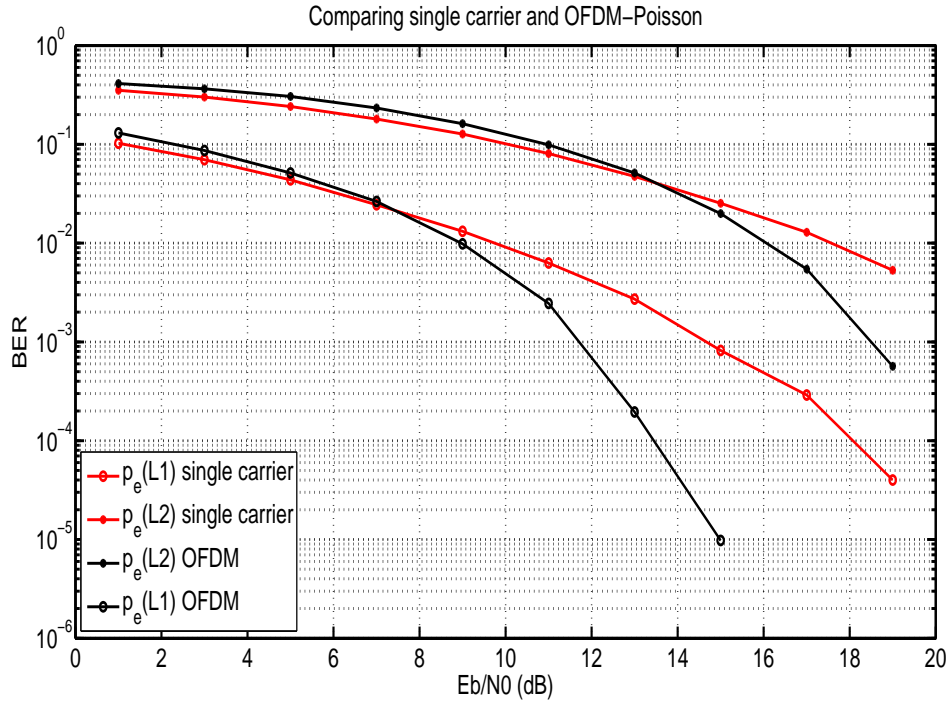
FIGURE 3.8: Comparing single carrier and OFDM at Poisson impulsive noise $N_i/N_o = 1$.

TABLE 3.3: Values of the parameters used in our second simulation

Parameter	value
$T_{impulse}/T_{symbol}$	1
p	0.3
λ	1
N_i/N_o	1
number of subcarriers	512
p_{e1}	10^{-3}
p_{e2}	10^{-1}

the bit loading algorithm targeting to protect two levels of data priority with certain BER for each level with the parameters shown in Table 3.3. Note that with the existence of the PLC channel and application of bit loading, the values of $d1$ and $d2$ are obtained by solving the BER expressions for the target error probabilities, and so in general we obtain non-uniform QAM constellations.

Shown in Fig. 3.9 and Fig. 3.10 are system simulations for both the Bernoulli and Poisson cases respectively achieving the required BER for both priority levels. In this simulation, the required BER was 10^{-1} and 10^{-3} for the low and high priority bits $p_e(L2)$
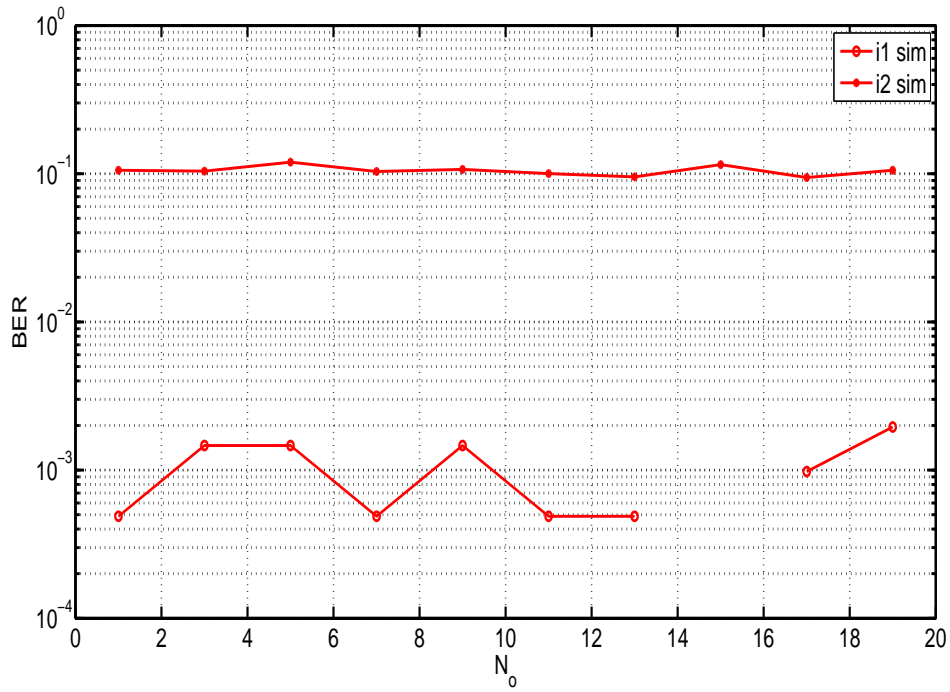
FIGURE 3.9: Achieving the required BER using the bit loading algorithm with Bernoulli impulsive noise.

and $p_e(L1)$, respectively and these required BER values may be varied according to the system specifications. Fig. 3.11 shows both the power allocated for each subcarrier as calculated by the bit loading algorithm, and its channel gain. Note that for the first set of simulations, we do not place a limit on the total energy budget. Placing such a limit will allow us to plot throughput curves against noise levels, as in some cases the limited energy budget will result in no transmission of some bits.
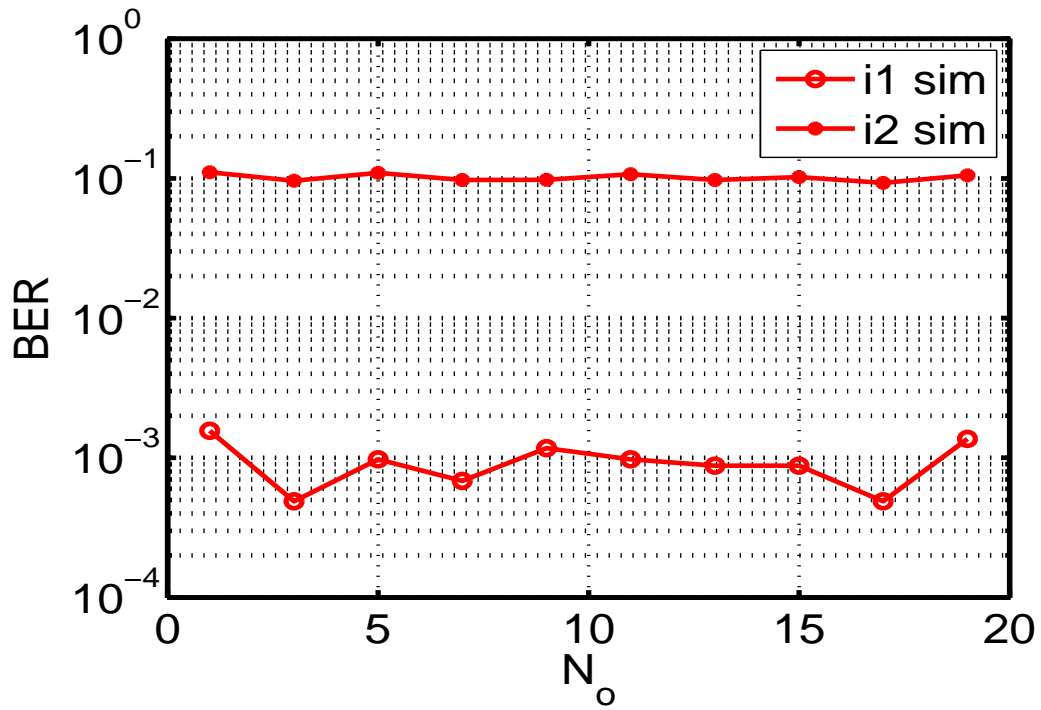
FIGURE 3.10: Achieving the required BER using the bit loading algorithm with Poisson impulsive noise.
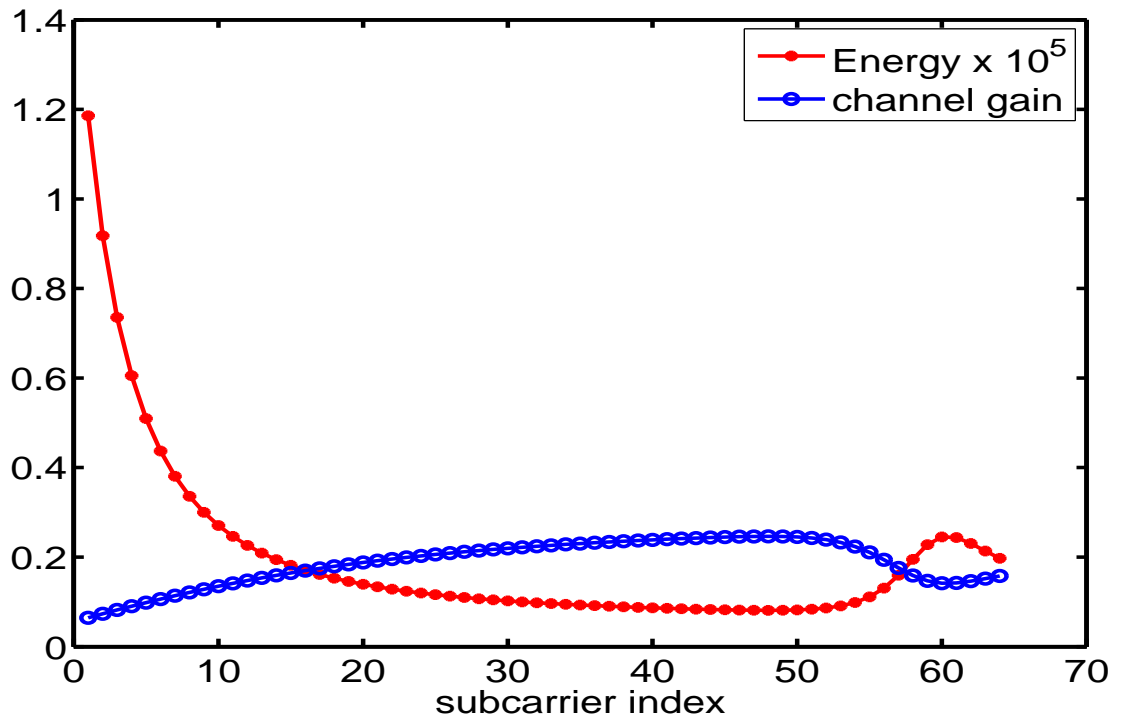

FIGURE 3.11: Comparing each subcarrier power with its channel gain at $N_o = 20$.

Chapter 4

MIMO PLC Systems: Space-Time Coding and Beamforming

4.1 Introduction

Although wireless systems have good performance within a room, their performance is degraded when the wireless signal has to pass through walls. So, utilizing the third wire of power line in a MIMO system enables increasing the coverage and capacity of PLC transmission [29]. Since 2008, large scale public measurements were started to get results on power line MIMO channels and noise characterization in several European countries. Several measurement results were published as presented in [30] and [31]. It was shown in [32] that different MIMO schemes can be applied to a PLC system. Spatial multiplexing for MIMO scheme can be used to provide a capacity gain through sending different data over different transmit antennas. Also, space-time or space-frequency block coding can be used to provide a diversity gain and overcome the channel fading, so Alamouti scheme is investigated in this work. However, it was stated in [29] that MIMO deployment in HV and MV lines are still limited due to the cost and problems in coupling of MIMO signals to power lines, so alternatives like optical fibers are used.
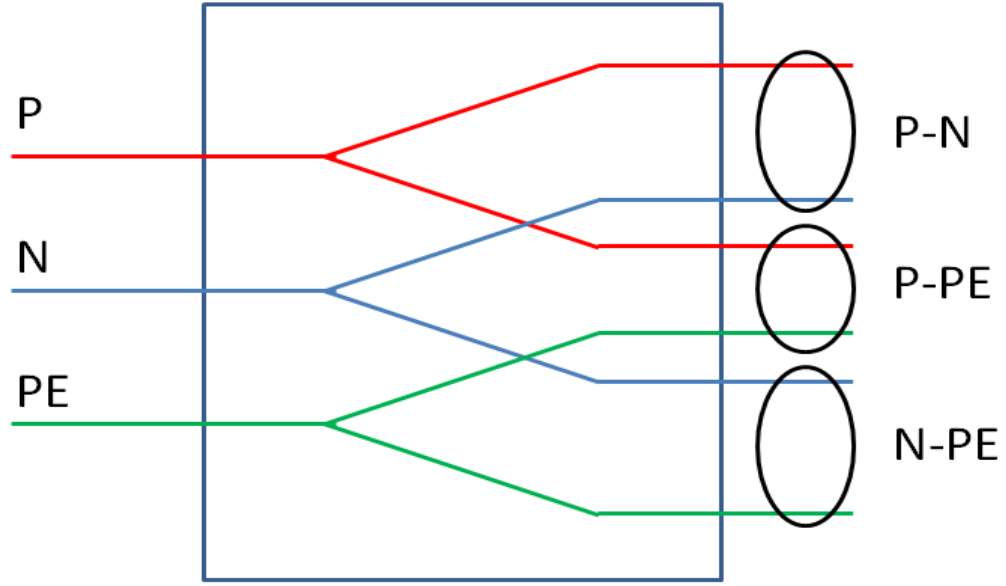
FIGURE 4.1: PLC Network.

4.1.1 MIMO PLC

The advantage of communication over power lines is that it can utilize all the three conductors (Positive, Negative, Protective Earth) to establish a multiple-input multiple-output (MIMO) system instead of using only one conductor for a single-input single-output (SISO) system. It was stated in [33] that speed beyond 200 Mbps can be reached with a 2×2 MIMO system. Also, it was stated in [34] that a 2×2 MIMO system with two differential feed and receive ports can be realized. Fig. 4.1 shows the splitter used for MIMO measurement of differential signals. Due to the Kirchhoff's laws, only two differential signals can be injected at the same time and at the receiver, the signal is observed between one conductor and a reference conductor. Alamouti space time block coding (STBC) [35] was used to obtain the transmit diversity. In this part, we use a channel model for 2x3 PLC channel which is the same model used in [36]. Here we extend UEP to four levels by using two different constellations sent from the transmitter, thus achieving two more different levels of data protection on symbol level added to the two levels of data protection on bit level through the Hierarical Modulation. Fig. 4.2 shows the PLC channel used for MIMO system simulations.
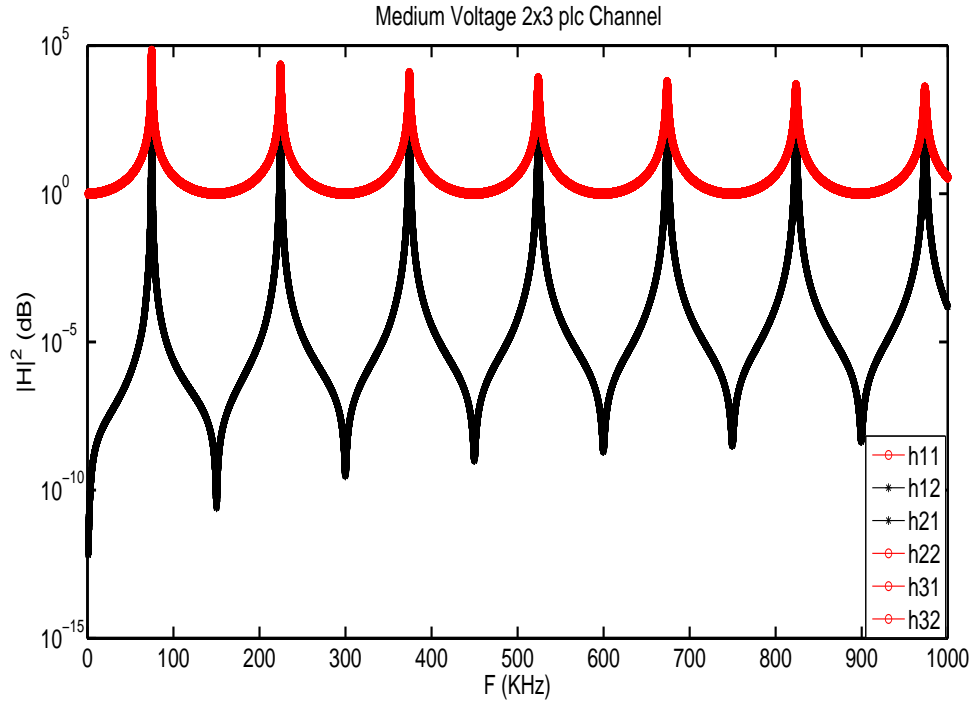
FIGURE 4.2: PLC 2x3 MIMO Channel Frequency Response.

In this work we present three cases for MIMO system applied to the hierarchical 4/16 QAM constellation with impulsive noise, which are 2×3 Alamouti system, 1×3 Maximal Ratio Combining system and we introduced an STBC to provide UEP through enhancing the protection of one symbol by sending it on the two time slots and sending the other symbol on one time slot only which is inspired by the codes in [37], however [37] has no explicit design for 2×3 codes. So x_1 will be more protected than x_2 as it will be transmitted from two different lines over the two time slots, while x_2 will only be transmitted from one line. And the received signal for this introduced code is given by

$$\begin{bmatrix} y_1 \\ y_2 \end{bmatrix} = \begin{bmatrix} h_{11} & h_{12} \\ h_{21} & h_{22} \end{bmatrix} \begin{bmatrix} x_1 & x_2 \\ 0 & x_1 \end{bmatrix} + \begin{bmatrix} n_1 \\ n_2 \end{bmatrix} \tag{4.1}$$

The annotation used in all figures through this chapter for analysis of the first Alamouti system is "Alam", for the second Maximal Ratio Combining system is "MRC" and for the third introduced STBC system is "Intro".

4.1.2 Alamouti System

Alamouti Space Time Block code is a scheme for coding across space and time. Addition of multiple antennas can introduce redundancy in space for Space Time coding and channel coding can introduce redundancy in time. Channel State Information (CSI) is not required by Alamouti at the transmitter. The Alamouti STBC scheme uses 2 antennas at the transmitter and m antennas at the receiver. The Alamouti scheme is the full rate code, because it transmits two symbols per two time instants [38].

Let the encoding matrix X, where the symbols x_1 and x_2 are mapped to two transmit antennas in two transmit time slots. The encoding matrix is given by

$$\begin{bmatrix} x_1 & x_2 \\ -x_2* & x_1* \end{bmatrix} \tag{4.2}$$

Now the received vector after first time slot will be,

$$\begin{bmatrix} y_{11} \\ y_{12} \end{bmatrix} = \begin{bmatrix} h_{11} & h_{12} \\ h_{21} & h_{22} \end{bmatrix} \begin{bmatrix} x_1 \\ x_2 \end{bmatrix} + \begin{bmatrix} n_{11} \\ n_{12} \end{bmatrix} \tag{4.3}$$

And the received vector after the second time slot will be,

$$\begin{bmatrix} y_{21} \\ y_{22} \end{bmatrix} = \begin{bmatrix} h_{11} & h_{12} \\ h_{21} & h_{22} \end{bmatrix} \begin{bmatrix} -x_2* \\ x_1* \end{bmatrix} + \begin{bmatrix} n_{21} \\ n_{22} \end{bmatrix} \tag{4.4}$$

We derive the BER equations for both of the Alamouti and MRC system and they are nearly the same as the equations derived earlier except for the signal to noise ratio (SNR) terms which are multiplied by the summation of channels' magnitudes to account for full diversity and multiplied also by a factor of 0.5 due to power division at the transmitter side for the Alamouti system. Hence,

$$SNR_{2 \times 1 \text{ Alamouti}} = 0.5 \times (|h_{11}|^2 + |h_{21}|^2) \times SNR_{|h|^2 = 1} \tag{4.5}$$

$$SNR_{2 \times 3 \text{ Alamouti}} = 0.5 \times (|h_{11}|^2 + |h_{12}|^2 + |h_{21}|^2$$
$$+ |h_{22}|^2 + |h_{31}|^2 + |h_{32}|^2) \times SNR_{|h|^2 = 1} \tag{4.6}$$
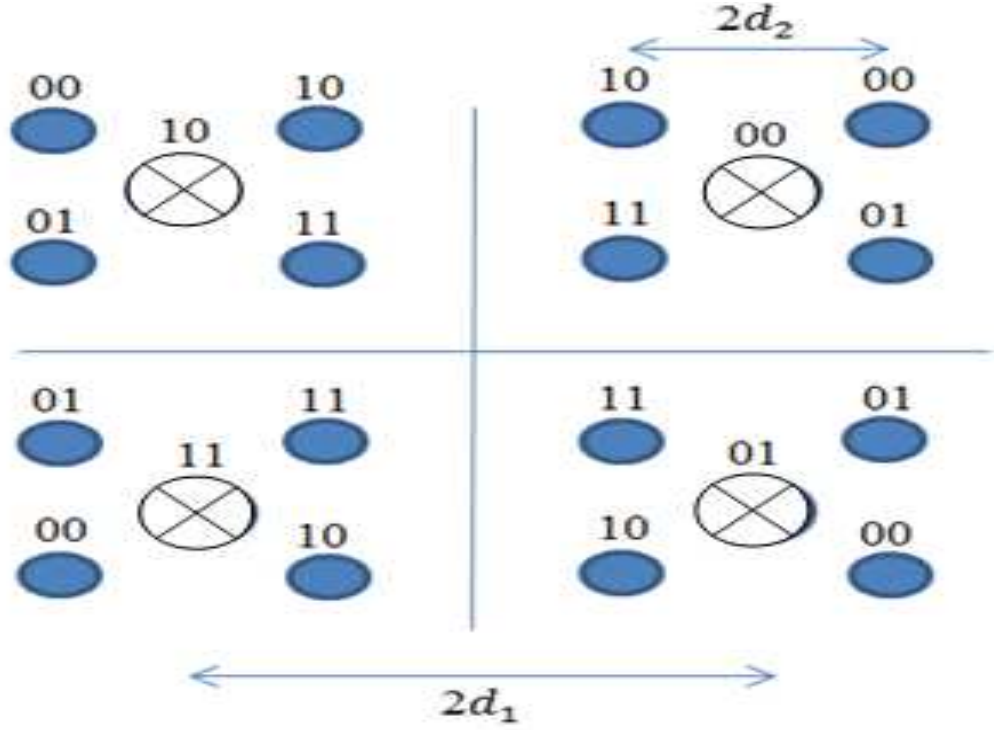
FIGURE 4.3: The first constellation for symbols S1.

where $SNR_{|h|^2 = 1}$ is the signal to noise ratio in case of channel with flat unity magnitude. Also taking into account different levels of protection at the symbol level using two different constellations, (d_1, d_2) and (d_3, d_4) for the first and second constellations S1 and S2 as shown in Fig. 4.3 and Fig. 4.4 respectively.

We achieve four levels of BER equations as follows

$$p_e(L1) \approx \frac{1}{4}\textbf{erfc}\left(\frac{d_1 - d_2}{\sqrt{N_o}}\right). \tag{4.7}$$

$$p_e(L2) \approx \frac{1}{2}\textbf{erfc}\left(\frac{d_2}{\sqrt{N_o}}\right) \tag{4.8}$$

$$p_e(L1) \approx \frac{1}{4}\textbf{erfc}\left(\frac{d_3 - d_4}{\sqrt{N_o}}\right). \tag{4.9}$$

$$p_e(L2) \approx \frac{1}{2}\textbf{erfc}\left(\frac{d_4}{\sqrt{N_o}}\right) \tag{4.10}$$
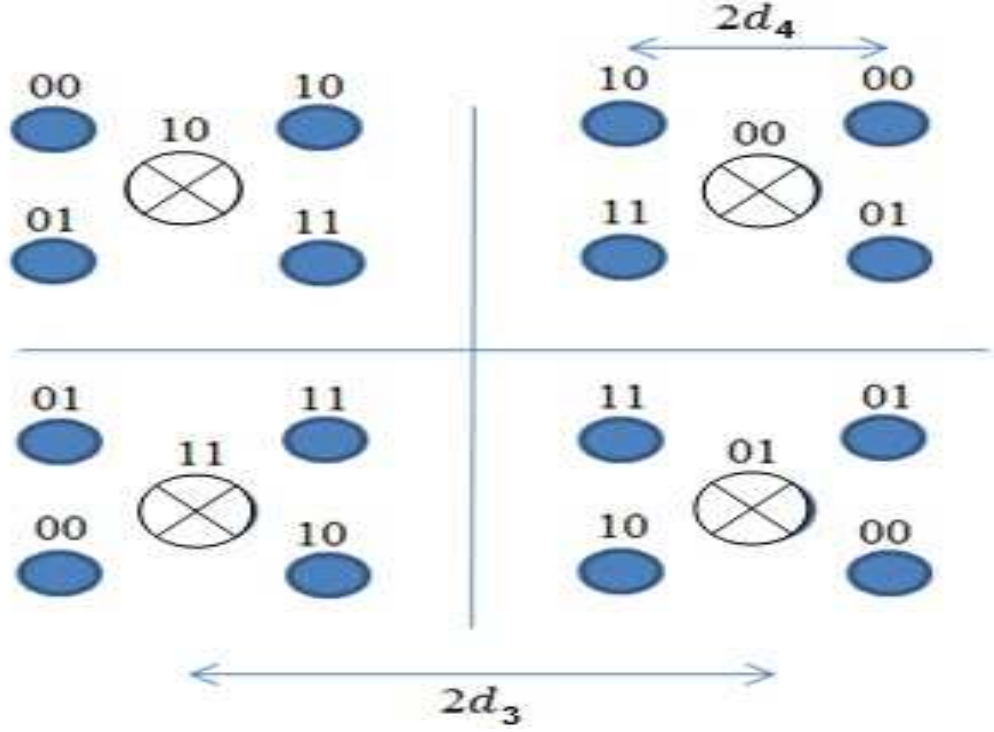
FIGURE 4.4: The Second constellation for symbols S2.

Also, in this work we present two cases for MIMO system applied to the hierarchical 4/16 QAM constellation in Bernoulli and Poisson impulsive noise which are 2×1 Alamouti system and 2×2 Alamouti system.

4.2 Beamforming

Space-time coding enables us to achieve diversity and coding gain over MIMO channels, however extra gain can be achieved using the channel knowledge information at the transmitter side. And for the case of power line communication, the channel is nearly fixed so the transmitter can have a priori channel knowledge. Using the optimum precoder forces the transmit antenna to send only the non-zero eignmodes [39]. [40] Let the singular-value decomposition (SVD) of H is

$$\mathbf{H} = \mathbf{U}\omega\mathbf{V}^{H} \tag{4.11}$$

The optimal transmit beamforming vector is

$$\mathbf{w_t}^{opt} = \mathbf{V} \tag{4.12}$$

The optimal receive beamforming vector is

$$\mathbf{w_r}^{opt} = \mathbf{U} \tag{4.13}$$

Then, the received signal $\mathbf{y}_r$ is

$$\mathbf{y}_r = \mathbf{H} \times \mathbf{w_t}^{opt} \times \mathbf{x}_t + \mathbf{n}_r \tag{4.14}$$

where $\mathbf{y}_r$ is the 3×1 received vector, $\mathbf{H}$ is the 3×2 channel matrix, $\mathbf{x}_t$ is the transmitted 2×1 data vector and $\mathbf{n}_r$ is the 3×1 noise vector.

And after the decoder at receiver

$$\mathbf{y} = \mathbf{w_r}^{opt} \times \mathbf{y}_r = \mathbf{\Lambda} \times \mathbf{x}_t + \mathbf{n} \tag{4.15}$$

where $\mathbf{\Lambda}$ is the eigenvalues diagonal matrix. So the MIMO channel is converted to SISO channel through the strongest eignmode beam forming.

4.3 Simulation Results

At first the MIMO Alamouti system was simulated for both cases 2x1 MIMO and 2x2 MIMO and comparison of the results with exact theoretical BER equations are shown in Fig. 4.5, Fig. 4.6, Fig. 4.7 and Fig. 4.8.

Then the MIMO 2×3 Alamouti system is simulated and Fig. 4.9 shows a comparison of the simulation results Pe with exact theoretical BER equations PT for both symbols $S1$ and $S2$ at both protection levels $L1$ and $L2$. The same comparison is done for the MIMO 1×3 MRC system and is shown in Fig. 4.10. It is clear that the BER approximations agree very well with the measured BER.

Then the 4 levels of BER for all the three MIMO systems are compared together at a fixed total transmitted power where the first three BER curves are overlapped as shown in Fig. 4.11 to have the same protection level so straight forward analysis for the three MIMO systems can be done through comparing the performance of the fourth level of BER. And we can compare the performance of the three systems through the fourth BER curve as shown in Fig. 4.12 which indicates the superiority of Alamouti
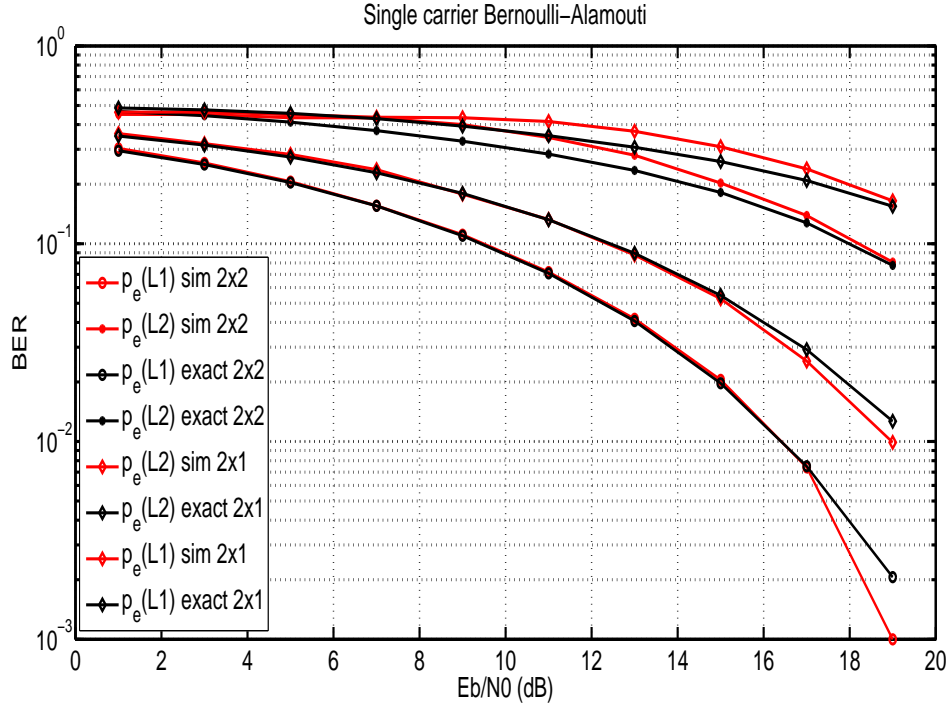
FIGURE 4.5: BER Analysis for Alamouti system 2×1 MIMO and 2×2 MIMO with Bernoulli noise model over single carrier. Simulation results "sim" are plotted along with theoritical results "exact".

FIGURE 4.6: BER Analysis for Alamouti system 2×1 MIMO and 2×2 MIMO with Poisson noise model over single carrier. Simulation results "sim" are plotted along with theoritical results "exact".
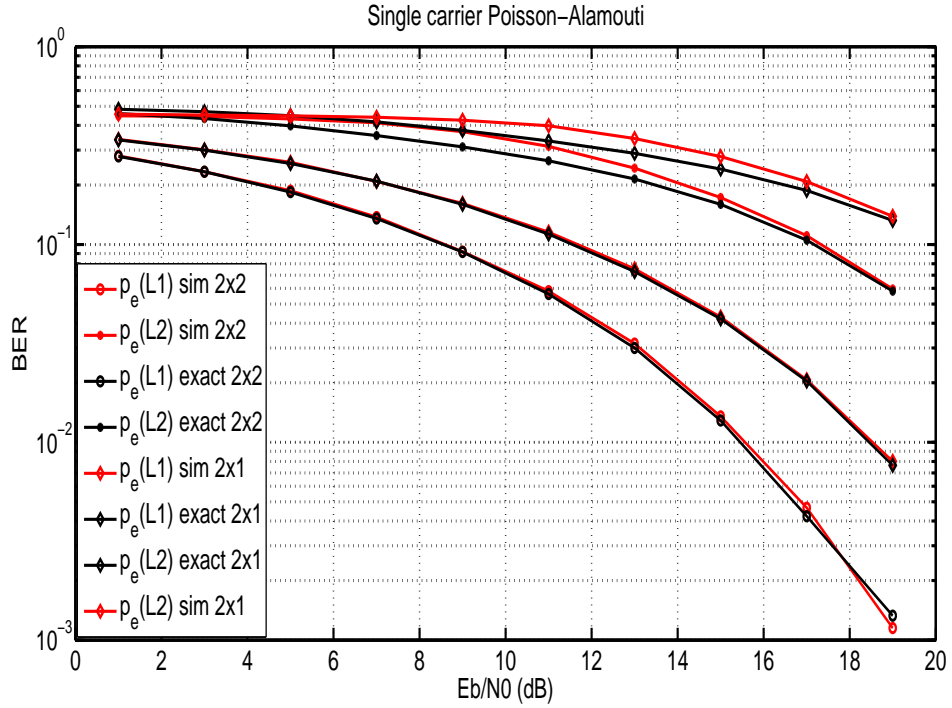
FIGURE 4.7: BER Analysis for Alamouti system 2×1 MIMO and 2×2 MIMO with Bernoulli noise model over OFDM. Simulation results "sim" are plotted along with theoritical results "exact".

FIGURE 4.8: BER Analysis for Alamouti system 2×1 MIMO and 2×2 MIMO with Poisson noise model over OFDM. Simulation results "sim" are plotted along with theoritical results "exact".

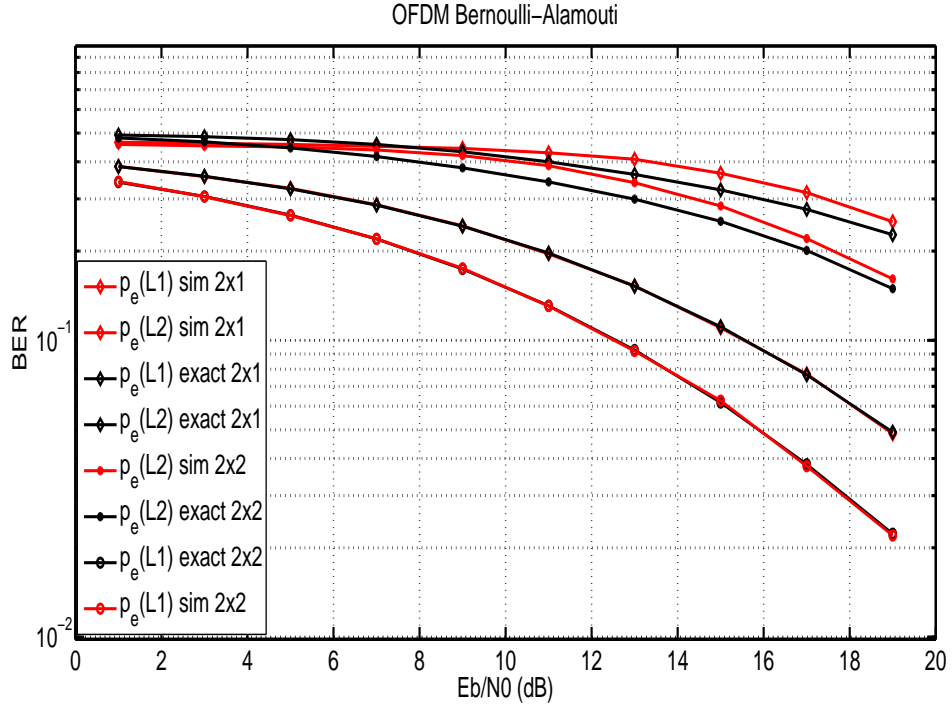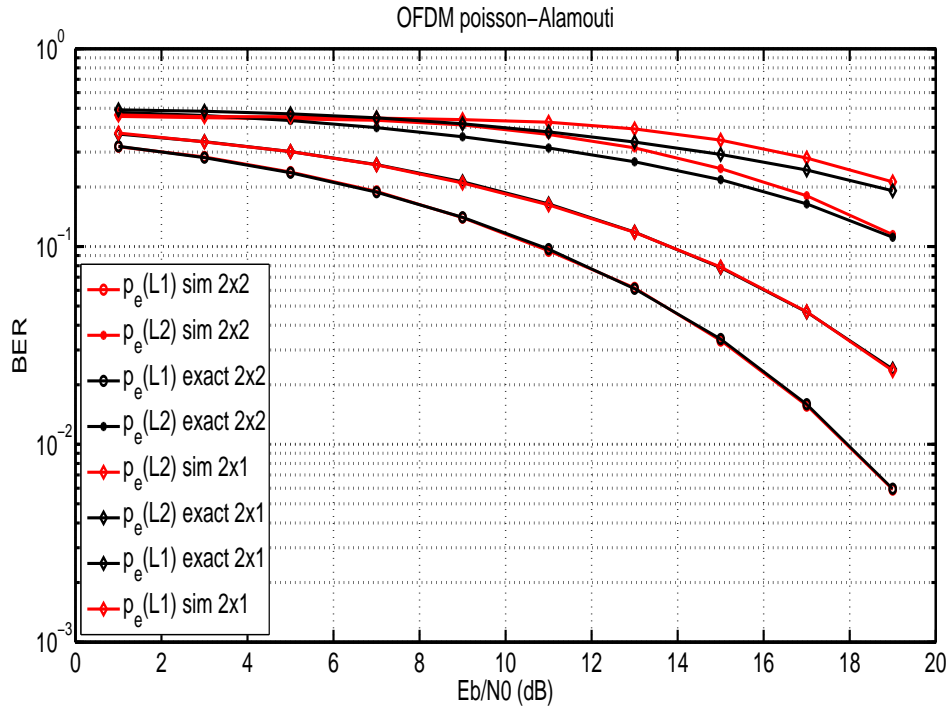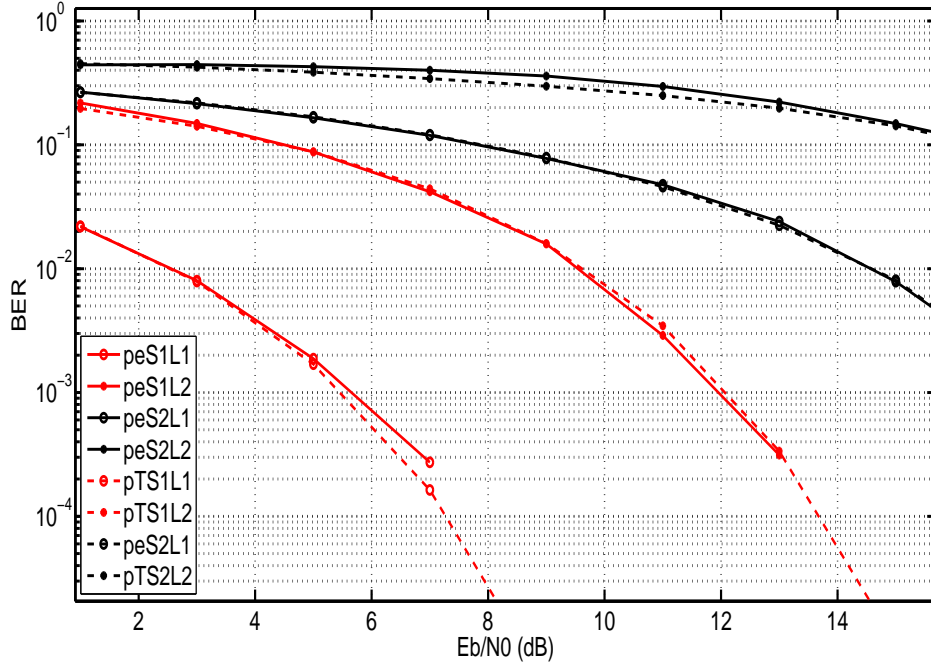FIGURE 4.9: BER Analysis for OFDM 2x3 Alamouti system
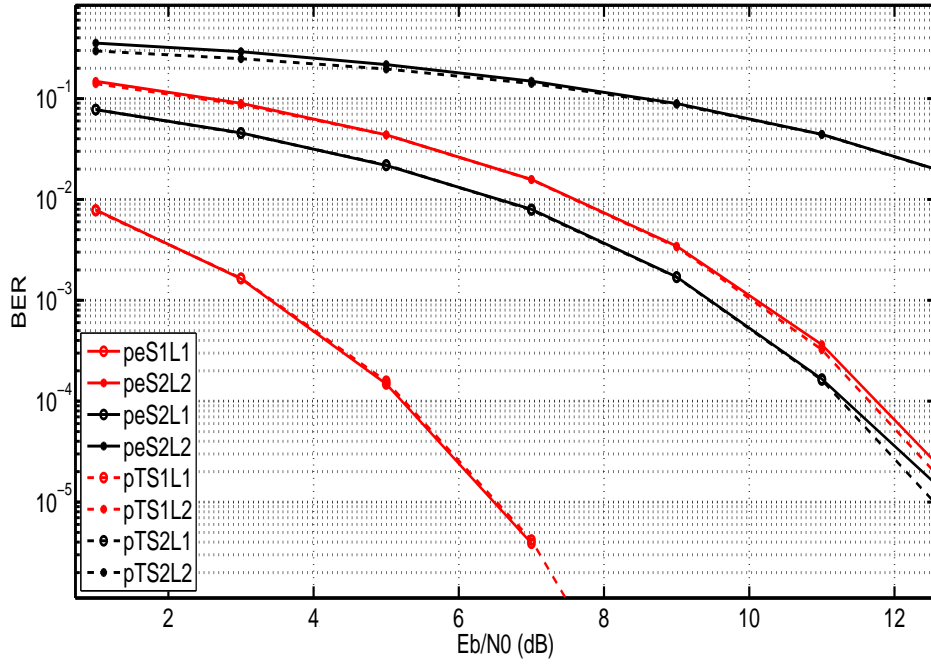
FIGURE 4.10: BER Analysis for OFDM 1x3 MRC system
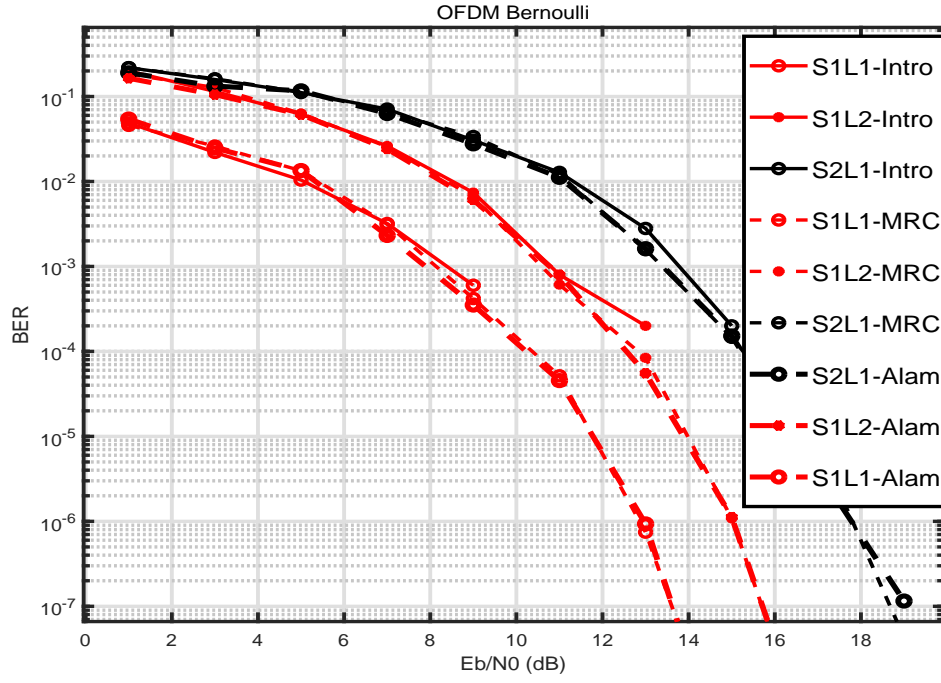
FIGURE 4.11: Showing perfect overlap of the first three levels of BER for the 2×3 Alamouti, the 1×3 MRC and the introduced STBC systems.

system. Also it is clear that the introduced code provides an extra level of UEP which is enhancing the most protected bit but it deteriorates the least protected bit.

Finally we apply the joint transmit and receive beamforming technique which results in more improvement of the system BER compared to Alamouti system as shown in Fig. 4.13. So that straight forward comparison indicates the superiority of the Beamforming system.

FIGURE 4.12: Comparing the fourth level of BER curves for the 2×3 Alamouti, the 1×3 MRC and the introduced STBC systems.

FIGURE 4.13: BER Analysis and comparison for Alamouti system "ala" and Beamforming system "bf".

Chapter 5

Conclusion and Future Work

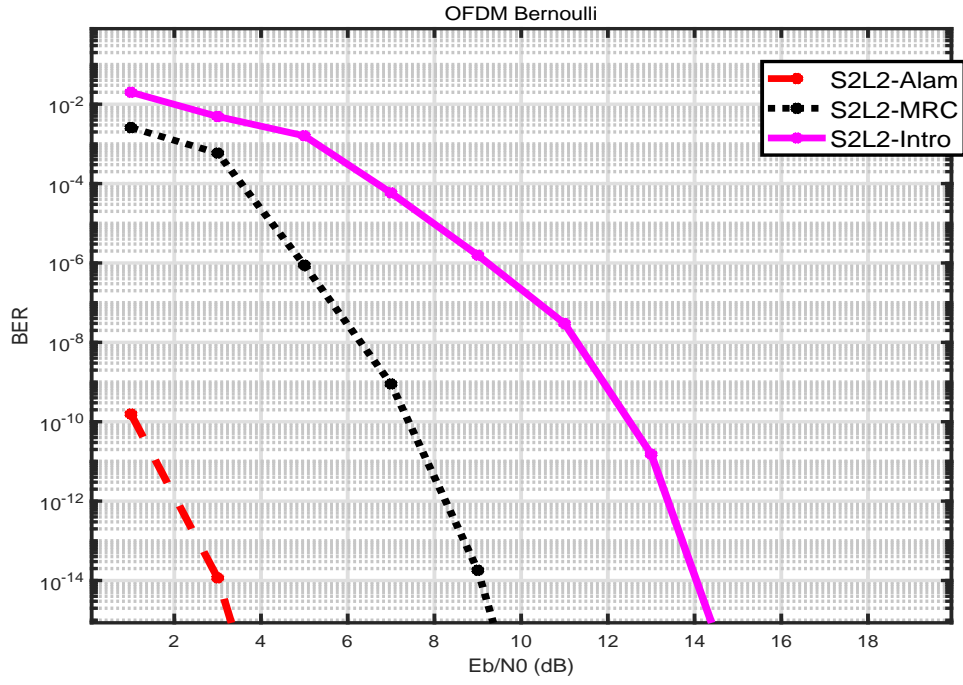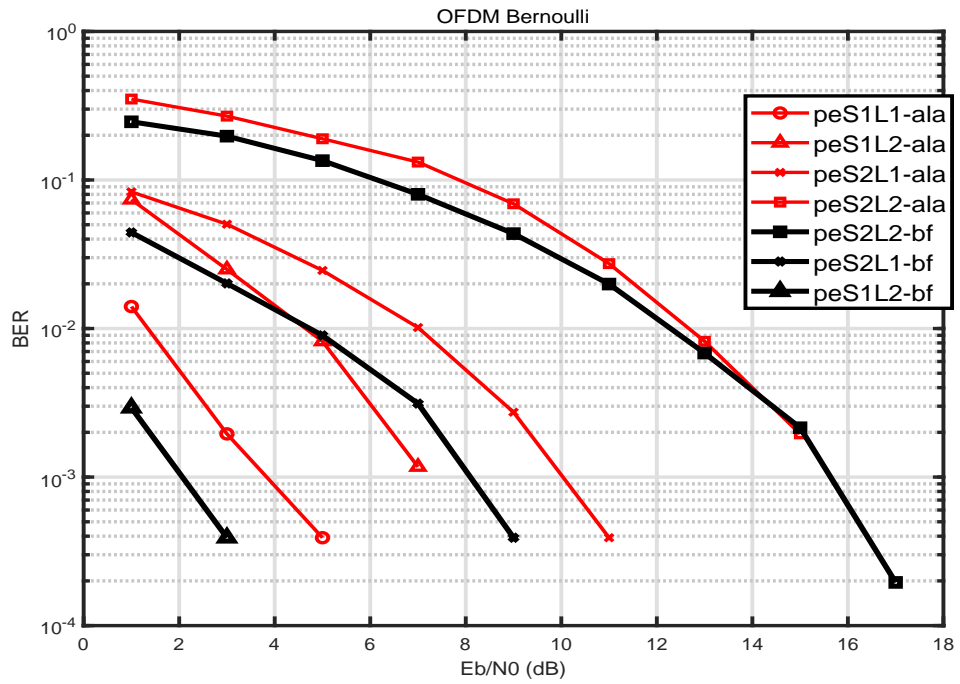## 5.1 Conclusion

In this work, we analyze and simulate UEP schemes over impulsive noise PLC channels with Bernoulli and Poisson arrivals for single- and multi-carrier systems in SISO and MIMO cases. We derive approximate error probability expressions and propose a bit loading algorithm for multi-carrier system to overcome PLC channel attenuation and achieve the desired BER for two levels of data protection. The approximate BER expressions enable practical application of the bit loading algorithm with negligible loss in performance. We also conclude that for strong impulsive noise, OFDM is better than single carrier at high SNR values. Utilizing the bit loading algorithm gives more protection for the highest priority level especially under a power constraint. Also, all the three conductors in power line (Positive, Negative, Protective Earth) can be utilized in a MIMO system and UEP is extended to 4 different levels through power scaling and using two different constellations at the same time. The usage of MIMO PLC channels in the three cases we study, which are 2×3 Alamouti system, 1×3 Maximal Ratio Combining system and an introduced STBC structure, allows more control over the protection of priority levels. These UEP levels can be controlled by selecting the appropriate STBC, power scaling and constellation parameters. Finally, precoding technique is used for joint beamforming at the transmitter and receiver to make use of the channel knowledge at transmitter which improves the BER.

5.2   Future Work

This work can be extended to study the system performance under different PLC channels and with different models for the impulsive noise for example narrowband PLC channel with dominant synchronous periodic impulsive noise. The 2×3 STBC which is based on [37] can be improved to achieve higher data rates also its detection technique may be improved instead of the used exhaustive search. The precoding technique can be further improved through power allocation of different streams according to their corresponding singular value in the Eigenvalues matrix. Future research can include the coupling effects between PLC conductors and the correlation among PLC MIMO channels. And different techniques for layered coding can be integrated with hierarchical modulation to give different protection levels. Also the noise models can be improved and compared to practical measurements through different power line network topologies.

Bibliography

[1] Wenye Wang, Yi Xu, and Mohit Khanna. "A survey on the communication architectures in smart grid". *The International Journal of Computer and Telecommunications Networking*, 55:3604–3629, 2011.

[2] Office of the National Coordinator for Smart Grid Interoperability. "NIST framework and roadmap for smart grid interoperability standards, release 2.0". In *NIST Special Publication 1108 R2*, 2012.

[3] U.S. DOE. "Communications requirements of smart grid technologies". http://energy.gov/sites/prod/files/gcprod/documents/Smart_Grid_Communications_Requirements_Report_10-05-2010.pdf, 2010.

[4] S. Galli, A. Scaglione, and Wang Zhifang. "For the grid and through the grid: The role of power line communications in the smart grid". In *Proceedings of the IEEE*, volume 99, pages 998–1027, June 2011.

[5] Joon-Myung Kang; Chang-Keun Park; Eun-Hee Kim; James Won-Ki Hong; Yong hun Lim; Seongho Ju; Moon-suk Choi; Bum-suk Lee; Duckhwa Hyun. "Design and implementation of network management system for power line communcation network". *2007 IEEE International Symposium on Power Line Communications and Its Applications*, 2007.

[6] https://www.esk.fraunhofer.de/en/research/projects/SMARTV2G.html.

[7] P. Mlynek, J. Misurec, and M. Koutny. "Random channel generator for indoor power line communication". In *Measurement Science Review*, volume 13, pages 206–213, 2013.

[8] M. Nassar, Jing Lin, Y. Mortazavi, A. Dabak, Il Han Kim, and B.L. Evans. "Local utility power line communications in the 3–500 khz band: Channel impairments, noise, and standards". *IEEE Signal Processing Magazine*, 29:116 – 127, 2012.

[9] M. Zimmermann and K. Dostert. "A multipath model for the powerline channel". *IEEE Transactions on Communications*, 50:553 – 559, 2002.

[10] S. Galli and T. Banwell. "A novel approach to the modeling of the indoor power line channel—part ii: Transfer function and its properties". *IEEE Transactions on Power Delivery*, 20:1869 – 1878, 2005.

[11] http://www.plc.uma.es/channels.htm.

[12] M. Zimmermann and K. Dostert. "Analysis and modeling of impulsive noise in broad-band powerline communications". *IEEE Transactions on Electromagnetic Compatibility*, 44:249 – 258, 2002.

[13] Jing Lin, M. Nassar, and B.L. Evans. "Impulsive noise mitigation in powerline communications using sparse bayesian learning". *IEEE Transactions on Selected Areas in Communications*, 31:1172 – 1183, 2013.

[14] M. Gotz, M. Rapp, and K. Dostert. "Power line channel characteristics and their effect on communication system design". *IEEE Communications Magazine*, 42:78 – 86, 2004.

[15] M. Katayama, T. Yamazato, and H. Okada. "A mathematical model of noise in narrowband power line communication systems". *IEEE Transactions on Selected Areas in Communications*, 24:1267 – 1276, 2006.

[16] M. Nassar, A. Dabak, Il Han Kim, T. Pande, and B.L. Evans. "Cyclostationary noise modeling in narrowband powerline communication for smart grid applications". In *2012 IEEE International Conference on Acoustics, Speech and Signal Processing (ICASSP)*, pages 3089 – 3092, 2012.

[17] Osama Mostafa; Karim G. Seddik; Ayman Elezabi. "Unequal error protection for impulsive noise channels in power line communications". *2016 International Symposium on Power Line Communications and its Applications (ISPLC)*, 2016.

[18] YH Ma, PL So, and E Gunawan. "Performance analysis of ofdm systems for broadband power line communications under impulsive noise and multipath effects". *IEEE Transactions on Power Delivery*, 20(2):674–682, 2005.

[19] F-X Coudoux, P Corlay, MG Gazalet, D Bueche, and M Slachciak. "On the use of hierarchical modulations for robust video transmission over power line medium". In *Power Line Communications and Its Applications, 2007. ISPLC'07. IEEE International Symposium on*, pages 482–486. IEEE, 2007.

[20] Keqian Yan, Kewu Peng, Fang Yang, Bingzhen Zhao, and Yirong Wang. "Performance improvement of g. hn system based on bit mapping technique". In *Power Line Communications and Its Applications (ISPLC), 2012 16th IEEE International Symposium on*, pages 150–154. IEEE, 2012.

[21] Pavan K Vitthaladevuni and M-S Alouini. "A recursive algorithm for the exact ber computation of generalized hierarchical qam constellations". *Information Theory, IEEE Transactions on*, 49(1):297–307, 2003.

[22] Werner Henkel and Khaled Hassan. "OFDM (DMT) bit and power loading for unequal error protection". In *OFDM-Workshop 2006*, pages 30–31, 2006.

[23] Dirk Hughes-Hartogs. "Ensemble modem structure for imperfect transmission media", May 23 1989. US Patent 4,833,706.

[24] Stephan Pfletschinger. *"Multicarrier modulation for broadband return channels in cable TV networks"*. Shaker, 2003.

[25] N. Al-Dhahir. "FIR channel-shortening equalizers for MIMO ISI channels". *IEEE Transactions on Communications 2001*, 2001.

[26] N. Al-Dhahir; J. M. Cioffi. "Efficiently computed reduced-parameter input-aided MMSE equalizers for ML detection: a unified approach". *IEEE Transactions on Information Theory*, 1996.

[27] D. D. Falconer; F. R. Magee. "Adaptive channel memory truncation for maximum likelihood sequence estimation". *The Bell System Technical Journal*, 1973.

[28] IEEE standard for broadband over power line networks: Medium access control and physical layer specifications, ieee std 1901-2010.

[29] A. Schwager, P. Pagani, and D.M. Schneider. "MIMO power line communications". *Communications Surveys and Tutorials, IEEE*, 2014.

[30] R. Hashmat, P. Pagani, A. Zeddam, and T. Chonavel. "MIMO communications for inhome PLC networks: Measurements and results up to 100 MHz". *Power Line Communications and Its Applications (ISPLC), 2010 IEEE International Symposium on*, 2010.

[31] D. Schneider, A. Schwager, J. Speidel, and A. Dilly. "Implementation and results of a MIMO PLC feasibility study". *Power Line Communications and Its Applications (ISPLC), 2011 IEEE International Symposium on*, 2011.

[32] Lothar Stadelmeier, Dietmar Schill, Andreas Schwager, Daniel Schneider, and Joachim Speidel. "MIMO for inhome power line communications". *Source and Channel Coding (SCC), 2008 7th International ITG Conference on*, 2008.

[33] F. Versolatto and A.M. Tonello. "A MIMO PLC random channel generator and capacity analysis". In *Power Line Communications and Its Applications (ISPLC), 2011 IEEE International Symposium on*, pages 66– 71. IEEE, 2011.

[34] R. Hashmat, P. Pagani, A. Zeddam, and T. Chonavel. "MIMO communications for inhome PLC networks: Measurements and results up to 100 MHz". In *Power Line Communications and Its Applications (ISPLC), 2010 IEEE International Symposium on*, pages 120– 124. IEEE, 2010.

[35] S. Alamouti. "A simple transmit diversity technique for wireless communications". *Selected Areas in Communications, IEEE Journal on*, 16:1451–1458, 1998.

[36] A.I. ; Papagiannis-G.K. ; ElSamadouny A. ; Al-Dhahir-N. Papadopoulos, T.A. ; Chrysochos. "MIMO modeling and data rates for medium-voltage narrowband-PLC in smart distribution grids". *Innovative Smart Grid Technologies Conference Europe (ISGT-Europe), 2014 IEEE PES*, pages 1–6, 2014.

[37] K. M. Z. Islam ; P. Rabiei ; N. Al-Dhahir ; S. N. Diggavi ; A. R. Calderbank. "Linear diversity-embedding STBC: design issues and applications". *IEEE Transactions on Communications 2009*, 2009.

[38] Jaipreet Kaur ; Maninder Lal Singh ; Rajdeep Singh Sohal. "Performance of alamouti scheme with convolution for MIMO system". *Recent Advances in Engineering and Computational Sciences (RAECS), 2015 2nd International Conference on*, 2015.

[39] H. Sampath ; A. Paulraj. "Linear precoding for space-time coded systems with known fading correlations". *IEEE Communications Letters, Volume: 6, Issue: 6, June 2002*, pages 239 – 241, 2002.

[40] https://www.ece.nus.edu.sg/stfpageelezhang.